



# **SOLUTION DENSITY MODELLING FOR SINGLE AND MIXED BASE METAL ELECTROLYTES AT IONIC LEVEL**

**Trevor Chagonda**

A research report submitted to the Faculty of Engineering and the Built Environment,  
University of the Witwatersrand, in partial fulfilment of the requirements for the degree of  
Master of Science in Metallurgical Engineering

**Johannesburg 2013**

## **DECLARATION**

I declare that this research report is my own unaided work. It is being submitted in partial fulfilment of the requirements of the degree of Master of Science in Metallurgical Engineering at the University of Witwatersrand, Johannesburg.

It has not been submitted before for any degree or examination to any other university.

.....

(Signature of Candidate)

..... **DAY OF** ..... **YEAR** .....

## ABSTRACT

Solution density modeling is important in hydrometallurgical processes as accurate predictions of single and mixed electrolytes can be used in the design of equipment and their sizing, heat transfer calculations and choosing of materials for construction.

This research project entails modeling of electrolyte solutions by extending the Laliberte and Cooper (compound level) model to ionic level where an electrolyte solution is modeled as a mixture of cations, anions and water molecules. This modeling predicts single and mixed electrolyte density as a function of electrolyte temperature in degrees Celsius; water, cation and anion apparent volumes in cubic centimeters; and their respective concentrations in the electrolyte as mass fractions.

The model was developed by fitting single electrolyte density data reported in literature using the least squares method in Microsoft Excel<sup>®</sup>. The following 26 single electrolyte solutions were used in the fitting exercise:  $\text{Al}_2(\text{SO}_4)_3$ ,  $\text{BaCl}_2$ ,  $\text{CaCl}_2$ ,  $\text{CdSO}_4$ ,  $\text{CoCl}_2$ ,  $\text{CuSO}_4$ ,  $\text{FeCl}_3$ ,  $\text{FeSO}_4$ ,  $\text{HCl}$ ,  $\text{HCN}$ ,  $\text{HNO}_3$ ,  $\text{K}_2\text{CO}_3$ ,  $\text{LiCl}$ ,  $\text{MgSO}_4$ ,  $\text{MnCl}_2$ ,  $\text{Na}_2\text{SO}_3$ ,  $\text{NaF}$ ,  $\text{NaI}$ ,  $\text{NaOH}$ ,  $(\text{NH}_4)_2\text{SO}_4$ ,  $\text{NiCl}_2$ ,  $\text{SrCl}_2$ ,  $\text{ZnCl}_2$ ,  $\text{ZnBr}_2$ ,  $(\text{NH}_4)_2\text{C}_2\text{O}_4$  and  $\text{KNO}_2$ . The above electrolytes attributed to the following ions:  $\text{Al}^{3+}$ ,  $\text{Ba}^{2+}$ ,  $\text{Ca}^{2+}$ ,  $\text{Cd}^{2+}$ ,  $\text{Co}^{2+}$ ,  $\text{Cu}^{2+}$ ,  $\text{Fe}^{3+}$ ,  $\text{Fe}^{2+}$ ,  $\text{H}^+$ ,  $\text{K}^+$ ,  $\text{Li}^+$ ,  $\text{Mg}^{2+}$ ,  $\text{Mn}^{2+}$ ,  $\text{Na}^+$ ,  $\text{NH}_4^+$ ,  $\text{Ni}^{2+}$ ,  $\text{Sr}^{2+}$ ,  $\text{Zn}^{2+}$ ,  $\text{SO}_4^{2-}$ ,  $\text{Cl}^-$ ,  $\text{CN}^-$ ,  $\text{NO}_3^-$ ,  $\text{CO}_3^{2-}$ ,  $\text{OH}^-$ ,  $\text{SO}_3^{2-}$ ,  $\text{Br}^-$ ,  $\text{F}^-$ ,  $\text{I}^-$ ,  $\text{C}_2\text{O}_4^{2-}$  and  $\text{NO}_2^-$ . This translated to a combination of at least 216 single electrolyte solutions which could be feasibly modeled, and a solution with at most 10 anions for mixed electrolytes, which is comparable with practical hydrometallurgical solutions.

A database of volumetric parameters was generated comprising a total of 18 cations and 12 anions. The validation of the developed model was done by predicting densities for both single and mixed electrolytes not used in the fitting exercise. The average density error i.e. the difference between experimental and model density for the single electrolyte solutions was  $22.62 \text{ kg m}^{-3}$  with a standard deviation of  $39.66 \text{ kg m}^{-3}$ . For the mixed electrolytes, the average density error was  $12.34 \text{ kg m}^{-3}$  with a standard deviation of  $24.48 \text{ kg m}^{-3}$ . These calculated errors translated to a maximum percentage average error of less than 4% for single electrolyte solutions and maximum average percentage of less than 3% for mixed electrolyte solutions.

## **ACKNOWLEDGEMENTS**

I wish to thank the following people for their support to this research project:

- My supervisor, Dr V. Sibanda and co-supervisor Professor S. Ndlovu, for their assistance, guidance and advice.
- Dr F. K. Crundwell for guidance, motivation and generous sharing of his vast knowledge of hydrometallurgy and model development.
- CM Solutions (Pty) Ltd for funding the research project and availing time throughout this research period.
- Ms K. Harris for editing support.
- My wife, Maureen, and daughter, Ruvarashe-Joy, for their encouragement, emotional support and ever believing in me. I love you both.

## **DEDICATION**

To my wonderful mother Stella Chagonda, a pillar of strength in my life. God bless and keep you always.

# CONTENTS

<b>DECLARATION</b>	<b>II</b>
<b>ABSTRACT</b>	<b>IV</b>
<b>ACKNOWLEDGEMENTS</b>	<b>V</b>
<b>DEDICATION</b>	<b>V</b>
<b>LIST OF FIGURES</b>	<b>VIII</b>
<b>LIST OF TABLES</b>	<b>XI</b>
<b>NOMENCLATURE</b>	<b>XII</b>
<b>1 INTRODUCTION</b>	<b>1</b>
1.1 BACKGROUND	1
1.2 MOTIVATION AND PROBLEM STATEMENT	2
1.3 AIM AND OBJECTIVES	4
1.4 RESEARCH QUESTIONS	5
1.5 HYPOTHESIS	6
1.6 RESEARCH PROJECT SCOPE	6
1.7 STRUCTURE OF THE REPORT	7
<b>2 LITERATURE REVIEW</b>	<b>8</b>
2.1 INTRODUCTION	8
<b>2.2 DENSITY MODELS IN LITERATURE</b>	<b>11</b>
2.2.1 EQUIVALENT CONCENTRATION MODEL	11
2.2.2 LINEAR MIXING RULE BASED ON MOLE FRACTION MODELS	12
2.2.3 NON LINEAR MIXING RULE MODELS	15
2.2.4 LINEAR MIXING RULE BASED ON MASS FRACTION MODEL	16
2.2.5 CONCLUSION	18
<b>3 RESEARCH METHODOLOGY</b>	<b>20</b>
3.1 INTRODUCTION	20

<b>3.2</b>	<b>DATA SOURCES</b>	<b>20</b>
<b>3.3</b>	<b>SELECTION OF DATA FOR FITTING AND MODEL TESTING</b>	<b>20</b>
<b>3.4</b>	<b>PROCESSING OF DATA FOR FITTING (MODEL DEVELOPMENT)</b>	<b>22</b>
3.4.1	PROCESSING DATA FOR MODEL DEVELOPMENT TO IONIC LEVEL	22
3.4.2	PROCESSING DATA FOR EXPANSION OF LALIBERTE AND COOPER DATA BASE	23
<b>3.5</b>	<b>MINIMIZATION OF THE SUM OF SQUARED ERRORS</b>	<b>24</b>
<b>3.6</b>	<b>STATISTICAL TESTING FOR DEVELOPED MODEL</b>	<b>24</b>
3.6.1	PROCESSING DATA FOR MODEL TESTING	24
3.6.2	STATISTICAL METHODS	25
<b>3.7</b>	<b>CONCLUSION</b>	<b>26</b>
<b>4</b>	<b>THEORETICAL DEVELOPMENT</b>	<b>28</b>
<b>4.1</b>	<b>INTRODUCTION</b>	<b>28</b>
<b>4.2</b>	<b>TOTAL ELECTROLYTE VOLUME MODELLING</b>	<b>28</b>
<b>4.3</b>	<b>DENSITY FUNCTION</b>	<b>29</b>
<b>4.4</b>	<b>WATER VOLUME MODELLING</b>	<b>29</b>
<b>4.5</b>	<b>IONIC VOLUME MODELLING</b>	<b>30</b>
<b>4.6</b>	<b>CONCLUSION</b>	<b>30</b>
<b>5</b>	<b>RESULTS AND DISCUSSIONS</b>	<b>32</b>
<b>5.1</b>	<b>INTRODUCTION</b>	<b>32</b>
<b>5.2</b>	<b>ESTIMATED PARAMETERS FOR SOLUTION DENSITY MODEL FOR 39 ADDED SALTS</b>	<b>32</b>
<b>5.3</b>	<b>DATA BASE FOR <math>c_0</math> TO <math>c_4</math> TERMS GENERATED FOR IONIC SPECIES</b>	<b>34</b>
<b>5.4</b>	<b>DATA FITNESS FOR SINGLE ELECTROLYTES USED IN THE FITTING EXERCISE</b>	<b>35</b>
<b>5.5</b>	<b>GRAPHICAL REPRESENTATION OF SINGLE ELECTROLYTES USED IN THE FITTING EXERCISE</b>	<b>37</b>
<b>5.6</b>	<b>DATA FITNESS FOR SINGLE ELECTROLYTES USED IN THE TESTING EXERCISE</b>	<b>38</b>
<b>5.7</b>	<b>GRAPHICAL REPRESENTATION OF SINGLE ELECTROLYTES USED IN THE TESTING EXERCISE</b>	<b>41</b>
<b>5.8</b>	<b>DATA AND GRAPHICAL FITNESS FOR SULFURIC ACID SOLUTIONS</b>	<b>42</b>

<b>5.9</b>	<b>DATA FITNESS FOR MIXED ELECTROLYTES SOLUTIONS</b>	<b>44</b>
<b>5.10</b>	<b>GRAPHICAL REPRESENTATION OF MIXED ELECTROLYTES FITS</b>	<b>48</b>
<b>6</b>	<b>CONCLUSIONS AND RECOMMENDATIONS</b>	<b>50</b>
<b>6.1</b>	<b>CONCLUSIONS</b>	<b>50</b>
<b>6.2</b>	<b>RECOMMENDATIONS</b>	<b>51</b>
<b>7</b>	<b>REFERENCES</b>	<b>53</b>
<b>APPENDIX A: SINGLE AND MIXED ELECTROLYTE DATA SOURCES</b>		
	<b>55</b>	
<b>APPENDIX B: SALTS USED IN THE MODEL DEVELOPMENT -</b>		
<b>FITTING EXERCISE</b>		<b>56</b>
<b>APPENDIX C: HANFORD ELECTROLYTE CONCENTRATIONS AS</b>		
<b>MASS FRACTIONS</b>		<b>57</b>
<b>APPENDIX D: GRAPHS FOR SINGLE ELECTROLYTE USED IN</b>		
<b>FITTING EXERCISE</b>		<b>58</b>
<b>APPENDIX E: GRAPHS FOR SINGLE ELECTROLYTE USED IN</b>		
<b>TESTING EXERCISE</b>		<b>62</b>
<b>APPENDIX F: GRAPHS FOR MIXED ELECTROLYTES</b>		<b>66</b>

## LIST OF FIGURES

Figure 1: Tree diagram of density model pairs for compound and ionic models .....	11
Figure 2: Plot of experimental vs. model density for $\text{Al}_2(\text{SO}_4)_3$ .....	37
Figure 3: Plot of experimental vs. model density for $\text{BaCl}_2$ .....	37
Figure 4: Plot of experimental vs. model density for $\text{CaCl}_2$ .....	38
Figure 5: Plot of experimental vs. model density for $\text{CdSO}_4$ .....	38
Figure 6: Plot of experimental vs. model density for $\text{CdCl}_2$ .....	41
Figure 7: Plot of experimental vs. model density for $\text{CoSO}_4$ .....	41
Figure 8: Plot of experimental vs. model density for $\text{CuCl}_2$ .....	41
Figure 9: Plot of experimental vs. model density for $\text{Fe}_2(\text{SO}_4)_3$ .....	41
Figure 10: Plot of experimental and model density vs. % wt. for $\text{H}_2\text{SO}_4$ at $0^\circ\text{C}$ .....	42
Figure 11: Plot of experimental and model density for $\text{H}_2\text{SO}_4$ at $0^\circ\text{C}$ up to a concentration of 30% acid in water.....	42
Figure 12: Plot of experimental and model density vs. % wt. for $\text{H}_2\text{SO}_4$ at $25^\circ\text{C}$ .....	43
Figure 13: Plot of experimental and model density for $\text{H}_2\text{SO}_4$ at $25^\circ\text{C}$ up to a concentration of 30% acid in water.....	43
Figure 14: Plot of experimental and model density vs. % wt. for $\text{H}_2\text{SO}_4$ at $60^\circ\text{C}$ .....	43
Figure 15: Plot of experimental and model density for $\text{H}_2\text{SO}_4$ at $60^\circ\text{C}$ up to a concentration of 30% acid in water.....	43
Figure 16: Plot of experimental and model density vs. % wt. for $\text{H}_2\text{SO}_4$ at $80^\circ\text{C}$ .....	43
Figure 17: Plot of experimental and model density for $\text{H}_2\text{SO}_4$ at $80^\circ\text{C}$ up to a concentration of 30% acid in water.....	43
Figure 18: Plot of experimental and model density vs. % wt. for $\text{H}_2\text{SO}_4$ at $100^\circ\text{C}$ .....	44
Figure 19: Plot of experimental and model density for $\text{H}_2\text{SO}_4$ at $100^\circ\text{C}$ up to a concentration of 30% acid in water.....	44
Figure 20: Plot of experimental vs. models densities for $\text{KCl}$ , $\text{MgCl}_2$ and $\text{CaCl}_2$ at $25^\circ\text{C}$ .....	48
Figure 21: Plot of experimental vs. models density for $\text{KCl}$ , $\text{MgCl}_2$ , $\text{CaCl}_2$ and $\text{NaCl}$ at $25^\circ\text{C}$ .	48
Figure 22: Plot of experimental vs. models density for $\text{NaCl}$ , $\text{Na}_2\text{SO}_4$ , $\text{NaOH}$ and $\text{NaCO}_3$ at $59^\circ\text{C}$ .....	48

Figure 23: Plot of experimental vs. models density for NaCl, NaBr, NaI, KCl, KBr and KI at 39°C .....	48
Figure 24: Plot of experimental vs. model density for NaCl and MgSO <sub>4</sub> at 25°C – 175°C .....	49
Figure 25: Plot of experimental vs. model density for Fe <sub>2</sub> (SO <sub>4</sub> ) <sub>3</sub> and KNO <sub>3</sub> at 25°C .....	49
Figure 26: Plot of experimental vs. model density for CoCl <sub>2</sub> .....	58
Figure 27: Plot of experimental vs. model density for CuSO <sub>4</sub> .....	58
Figure 28: Plot of experimental vs. model density for FeCl <sub>3</sub> .....	58
Figure 29: Plot of experimental vs. model density for FeSO <sub>4</sub> .....	58
Figure 30: Plot of experimental vs. model density for HCl .....	58
Figure 31: Plot of experimental vs. model density for HCN .....	58
Figure 32: Plot of experimental vs. model density for HNO <sub>3</sub> .....	59
Figure 33: Plot of experimental vs. model density for K <sub>2</sub> CO <sub>3</sub> .....	59
Figure 34: Plot of experimental vs. model density for LiCl .....	59
Figure 35: Plot of experimental vs. model density for MgSO <sub>4</sub> .....	59
Figure 36: Plot of experimental vs. model density for MnCl <sub>2</sub> .....	59
Figure 37: Plot of experimental vs. model density for NaSO <sub>3</sub> .....	59
Figure 38: Plot of experimental vs. model density for NaF .....	60
Figure 39: Plot of experimental vs. model density for NaI .....	60
Figure 40: Plot of experimental vs. model density for NaOH .....	60
Figure 41: Plot of experimental vs. model density for (NH <sub>4</sub> ) <sub>2</sub> SO <sub>4</sub> .....	60
Figure 42: Plot of experimental vs. model density for NiCl <sub>2</sub> .....	60
Figure 43: Plot of experimental vs. model density for SrCl <sub>2</sub> .....	60
Figure 44: Plot of experimental vs. model density for ZnCl <sub>2</sub> .....	61
Figure 45: Plot of experimental vs. model density for ZnBr <sub>2</sub> .....	61
Figure 46: Plot of experimental vs. model density for (NH <sub>4</sub> ) <sub>2</sub> C <sub>2</sub> O <sub>4</sub> .....	61
Figure 47: Plot of experimental vs. model density for KNO <sub>2</sub> .....	61
Figure 48: Plot of experimental vs. model density for FeCl <sub>2</sub> .....	62
Figure 49: Plot of experimental vs. model density for K <sub>2</sub> SO <sub>4</sub> .....	62
Figure 50: Plot of experimental vs. model density for KCl .....	62
Figure 51: Plot of experimental vs. model density for KNO <sub>3</sub> .....	62
Figure 52: Plot of experimental vs. model density for KOH .....	62
Figure 53: Plot of experimental vs. model density for Li <sub>2</sub> SO <sub>4</sub> .....	62

Figure 54: Plot of experimental vs. model density for $\text{MgCl}_2$ .....	63
Figure 55: Plot of experimental vs. model density for $\text{MnSO}_4$ .....	63
Figure 56: Plot of experimental vs. model density for $\text{Na}_2\text{CO}_3$ .....	63
Figure 57: Plot of experimental vs. model density for $\text{Na}_2\text{SO}_4$ .....	63
Figure 58: Plot of experimental vs. model density for $\text{NaBr}$ .....	63
Figure 59: Plot of experimental vs. model density for $\text{NaCl}$ .....	63
Figure 60: Plot of experimental vs. model density for $\text{NaNO}_3$ .....	64
Figure 61: Plot of experimental vs. model density for $\text{NH}_4\text{Cl}$ .....	64
Figure 62: Plot of experimental vs. model density for $\text{NiSO}_4$ .....	64
Figure 63: Plot of experimental vs. model density for $\text{ZnSO}_4$ .....	64
Figure 64: Plot of experimental vs. model density for $\text{Cd}(\text{NO}_3)_2$ .....	64
Figure 65: Plot of experimental vs. model density for $\text{HBr}$ .....	64
Figure 66: Plot of experimental vs. model density for $\text{Mg}(\text{NO}_3)_2$ .....	65
Figure 67: Plot of experimental vs. model density for $\text{Co}(\text{NO}_3)_2$ .....	65
Figure 68: Plot of experimental vs. model density for $\text{NH}_4\text{NO}_3$ .....	65
Figure 69: Plot of experimental vs. model density for $\text{Ca}(\text{NO}_3)_2$ .....	65
Figure 70: Plot of experimental vs. model density for $\text{Fe}_2(\text{SO}_4)_3$ and $\text{NaNO}_3$ at $25^\circ\text{C}$ .....	66
Figure 71: Plot of experimental vs. model density for $\text{Fe}_2(\text{SO}_4)_3$ and $\text{KBr}$ at $25^\circ\text{C}$ .....	66
Figure 72: Plot of experimental vs. model density for $\text{Fe}_2(\text{SO}_4)_3$ and $\text{NaBr}$ at $25^\circ\text{C}$ .....	66
Figure 73: Plot of experimental vs. models density for Hanford waste solutions at $25^\circ\text{C}$ .....	66
Figure 74: Plot of experimental vs. model density for $\text{H}_2\text{SO}_4$ and $(\text{NH}_4)_2\text{SO}_4$ at $-30^\circ\text{C}$ to $80^\circ\text{C}$ .....	67
Figure 75: Plot of experimental vs. model density for $\text{H}_2\text{SO}_4$ , $(\text{NH}_4)_2\text{SO}_4$ and $\text{NH}_4\text{NO}_3$ at $-30^\circ\text{C}$ to $80^\circ\text{C}$ .....	67
Figure 76: Plot of experimental vs. model density for $\text{NH}_4\text{Al}(\text{SO}_4)_2$ at $40^\circ\text{C}$ – $80^\circ\text{C}$ .....	67
Figure 77: Plot of experimental vs. model density for $\text{K}_3\text{Fe}(\text{CN})_6$ at $40^\circ\text{C}$ – $80^\circ\text{C}$ .....	67

## LIST OF TABLES

Table 1.1: Structure of research project report. ....	7
Table 5.1: Values of $c_0$ to $c_4$ for 39 salts from Equation 14. ....	33
Table 5.2: Generated apparent volume terms for ionic species .....	34
Table 5.3: Electrolytes used in the fitting exercise and error analysis.....	36
Table 5.4: Electrolytes used in the testing exercise and error analysis.....	39
Table 5.5: Largest error analysis for single electrolyte solutions .....	40
Table 5.6: Mixed electrolyte used for model testing and error analysis .....	45
Table 5.7: Largest error analysis for mixed electrolyte solutions.....	45
Table 5.8 Hanford waste models densities and error analysis results.....	47

## NOMENCLATURE

$\alpha$	Quadratic coefficient
$a_A$	Anion deviation parameter
$a_C$	Cation deviation parameter
$-\alpha$	Parameter accounting for water volume deviation
B	Quadratic coefficient
$c_0$	Empirical constant
$c_1$	Empirical constant
$c_2$	Empirical constant
$c_3$	Empirical constant
$c_4$	Empirical constant
$m_{H_2O}$	Mass flow rate of water (kg/h)
$M_i$	Molar mass of species 1 (g)
$m_{\text{solutes}}$	Mass flow rate of solute (kg/h)
$n$	Stoichiometric coefficient
$\rho$	Total electrolyte density (g/cm <sup>3</sup> )
$\rho_{H_2O}$	Density of water (g/cm <sup>3</sup> )
$\rho_{\text{solution}}$	Density of solution (g/cm <sup>3</sup> )
$t$	Temperature in degrees Celsius (°C)
$V$	Total electrolyte volume (cm <sup>3</sup> )
$v_{ms}$	Total specific volume (cm <sup>3</sup> )
$V_A^0$	Anion molar volume (cm <sup>3</sup> )
$V_C^0$	Cation molar volume (cm <sup>3</sup> )
$V_S^0$	Dissolved salt volume (cm <sup>3</sup> )
$V_w^0$	Water volume (cm <sup>3</sup> )
$v_{app,I}$	Apparent specific volume of species I (cm <sup>3</sup> /g)
$V_{elec}$	Salt apparent volume (cm <sup>3</sup> )
$v_{H_2O}$	Specific volume of water (cm <sup>3</sup> /g)
$V^{inf}$	True partial molar volume at infinity dilution (cm <sup>3</sup> )

$V_w$	Water apparent volume (cm <sup>3</sup> )
$w_{H_2O}$	Water mass fraction
$w_i$	Mass fraction of species i
$x_{elec}$	Salt apparent molality (mol/kg)
$x_i$	molar fraction of species i
$x_w$	Water apparent molality (mol/kg)
$w_{cation}$	Cation mass fraction
$w_{anion}$	Anion mass fraction
$v_{cation}$	Cation apparent volume (cm <sup>3</sup> )
$v_{anion}$	Anion apparent volume (cm <sup>3</sup> )

# 1 INTRODUCTION

## 1.1 BACKGROUND

The calculation of solution densities is important in hydrometallurgical design and operations. This is because flows in plants, equipment inventory and sizing are based on volume – which is a function of density. Equipment critical in the design of a hydrometallurgical plant includes tanks, pipes and pumps with parameters such as size, power and materials of construction being affected and determined by the density and volume of solution flowing through the equipment (Laliberte *et al.* 2004).

The calculation of density of any solution requires accurate total mass and volume of the solution. Total mass is a total of the masses of the dissolved cations, anions and water, which is fairly easy to determine owing to the advanced analytical instruments used in qualitative and quantitative analysis such as the XRF and ICP spectrometers. In addition, since mass is not affected by temperature changes, this makes its calculation over a temperature range easy as it remains constant. Total volume is a total of the volumes of the dissolved cations, anions and water and, since volume is affected by both temperature and concentration; its calculation is more difficult. Thus, mathematical modelling is employed in this research project to correlate volumetric changes to concentration and temperature changes in a solution.

Since salts dissociate to their building ions, a model based on predicting volumetric properties as a function of solution temperature and concentration of cations, anions and water species was developed. The importance of such a model is that it will be useful in the hydrometallurgical industry as important processes such as leaching produce mixed solutions of dissolved cations and anions in aqueous media. Such mixtures have different ions at different concentrations resulting in complicated interactions between cations/anions and water molecules in the solution, thus making total solution volume difficult to calculate (Reynolds *et al.* 2008).

An example of where densities of slurries and solutions were used as a process control parameter and tank utilization evaluations, is in the design of the Hanford waste treatment and

immobilization plant in the United States of America (Gephart *et al.* 2010). The Hanford waste treatment plant treats radioactive nuclear waste to produce stable products. The nuclear waste contains sodium salts including nitrates, carbonates, nitrites, sulphates, phosphates, hydroxides and aluminates. Due to the large concentrations and diverse species in the waste, finding a model that can accurately predict densities of such complex solutions as a function of temperature and concentration was important. Availability of the model done by Laliberte and Cooper made the design of a suitable plant to contain such solutions during the treatment process manageable (Carter *et al.* 2007). Though the Laliberte and Cooper model was fairly successful, the calculations were found to be complex as ionic species concentration results had to be converted to possible dissolved compounds before density calculations are done.

The developed ionic model will be used to motivate for a density simulator which can be used in the metallurgical simulation package Cycad Processes™ just as Clarke's model has been successfully used in Aspen Properties™, a software package used in the chemical and metallurgical industries (Redlich *et al.* 1940). The developed density simulator and its incorporation into Cycad Processes® simulation package will be useful in predicting volumetric properties of hydrometallurgical solutions for accurate sizing of the plant equipment suitable for unique hydrometallurgical processes.

In this research project, models in literature for mixed electrolyte density modelling to date are considered for further development. This involved examination of a number of models with a particular focus on extending the model developed by Laliberte and Cooper (Laliberte *et al.* (2004) for the densities of aqueous components to describe the density of aqueous solutions based on their building ionic species.

## 1.2 MOTIVATION AND PROBLEM STATEMENT

Due to the importance of solution densities in the hydrometallurgical industry, accurate prediction of density for mixed electrolyte solutions is imperative, especially in designing and sizing of metallurgical plants and process optimization.

To date a number of models for predicting mixed electrolyte density have been developed; unfortunately few have been evaluated; and most have limited accuracy for practical use. Their limitations are attributed to factors such as:

- (i) Complexity to calculate due to complicated speciation of ionic species in solution such as in the Pitzer model (Kumar *et al.* 1986).
- (ii) Limited scope of media of the Dixon model (Dixon *et al.* 2004) where only one medium such as sulfate or chloride can be predicted at a time. This may not work in mixed electrolytes.
- (iii) Limited prediction capabilities such as the Horsak and Slama model where only single electrolyte densities can be predicted. Thus it is not useful for more practical mixed electrolyte solutions (Horsak *et al.* 1986).
- (iv) Limited assumptions such as the Laliberte and Cooper model (Laliberte *et al.* 2004) where an electrolyte is modeled as a dissolved compound while in real practice dissociation to cations and anions takes place for salts in water.

These are some of the limitations in the models developed to date. Improved understanding of these models through a review of their weaknesses and derivations is discussed in the literature review section for selected models. Emphasis was given to the Laliberte and Cooper model for further development where an electrolyte was modeled as a mixture of cations, anions and water in solution.

Validation of the developed model will be done by predicting single and mixed electrolyte solutions by the developed model and then comparing the densities to the experimental densities. In addition, the developed model will be tested and validated by predicting the density of sulfuric acid. Sulfuric acid was chosen because: (i) it is one of the most important and used reagents in hydrometallurgy for leaching of mineral ores and (ii) it has two possible dissociation mechanisms which are either dissociation to the hydrogen and the per-sulfate ions or dissociation to the hydrogen and the sulfate ions respectively. Due to these two possible

dissociation mechanisms, complete dissociation to the hydrogen and sulfate ions will be assumed when testing and validating the developed model. This assumption will give an indication as to what extent sulfuric acid will dissociate completely as a function of concentration and temperature.

Note that due to these possible dissociations, sulfuric acid will be excluded in the model development exercise, however will be used in the validation exercise as a robust testing for the developed model.

### 1.3 AIM AND OBJECTIVES

The aim of this research project is to develop a model that will be able to accurately predict the density of single and mixed electrolyte solutions and be of practical use in the hydrometallurgical industry. This will be achieved by extending the Laliberte and Cooper model for solution density calculations to account for cations, anions and water molecules in an electrolyte. At ionic level flexibility is expected to be achieved as analytical instruments to date have the ability to qualitatively and quantitatively measure ions in electrolyte solutions.

The objectives of this research project are:

- (i) To extend the existing Laliberte and Cooper model from the compound level to ionic level where a dissolved salt will be flexibly modeled as a mixture of cations, anions and water.
- (ii) To compile a database of constants for software development of a density simulator in Cycad Processes®.
- (iii) To evaluate the predicting capability of the developed model for practical application in the hydrometallurgical industry.

- (iv) Using the developed model during validation, test to what extent the assumption for complete dissociation applies to sulfuric acid as temperature and concentration vary.
- (v) To increase the Laliberte and Cooper data base by estimating parameters for salts not done by Laliberte and Cooper. A total of 39 salts were considered in addition to the 59 salts worked on by Laliberte and Cooper (Laliberte *et al.* 2004).

#### 1.4 RESEARCH QUESTIONS

The following research questions will be explored:

- (i) To what extent does the developed model predict single and mixed electrolyte densities?
- (ii) To what extent does complete dissociation of a salt compound to its respective ionic constituents affect total solution density?
- (iii) To what extent does temperature and concentration affect electrolyte densities?
- (iv) To what extent does the Laliberte and Cooper model compare to the developed model and how flexible is the developed model?
- (v) In what range of concentration and temperature is complete dissociation true for sulfuric acid:  $H_2SO_{4aq} \rightarrow 2H^+_{aq} + SO_4^{2-}_{aq}$ ?

## 1.5 HYPOTHESIS

Extending the Laliberte and Cooper model to model an electrolyte solution as a mixture of cations, anions and water will result in a more accurate and flexible way to predict densities of mixed electrolyte solutions.

## 1.6 RESEARCH PROJECT SCOPE

The research project was executed in the following way:

1. Single and mixed electrolyte density data was compiled into Excel<sup>®</sup> spreadsheets; and the respective ionic mass fraction contribution was calculated.
2. The Laliberte and Cooper equation was developed to account for ionic species in an electrolyte; and the equations were built into Microsoft Excel<sup>®</sup> spreadsheets.
3. Using the least squares method the error between experimental and model densities was minimized.
4. A data base of the generated parameters from the above minimization process was compiled.
5. Using the generated parameters, densities of single electrolyte solutions were generated and compared to their corresponding experimental densities.
6. Using the generated parameters, densities of mixed electrolyte solutions were generated and compared to their corresponding experimentally measured densities.

7. The generated parameters for hydrogen proton and sulfate ion were tested on how well and to what extent they are able to predict sulfuric acid density with respect to concentration and temperature.
8. The fittings were compared using statistical methods for curve fittings.

## 1.7 STRUCTURE OF THE REPORT

This research report is made up of seven sections:

Table 1.1: Structure of research project report.

Chapter 1	Introduction	This section includes the motivation, problem statement, aim and objectives, research questions, hypothesis and scope of research project
Chapter 2	Literature review	This section examines density models in literature, and positions this research project within that body of knowledge
Chapter 3	Research methodology	This section examines the sources of selection of data, along with the processing of data for model development, minimization of the sum of squared errors, and statistical testing of the developed model
Chapter 4	Theoretical development	This section covers total electrolyte volume modeling, density function, and water and ionic volume modeling
Chapter 5	Results and discussions	This section provides the database for $c_0$ to $c_4$ terms generated, presents data fitness and graphical representation for single and mixed electrolytes (both those used in the fitting exercise and those not), as well as for sulfuric acid solutions
Chapter 6	Conclusions and recommendations	This section draws conclusions with reference to the existing body of knowledge, and makes recommendations for further development and testing
Chapter 7	References	This section contains references used in the text as well as additional sources consulted

## 2 LITERATURE REVIEW

### 2.1 INTRODUCTION

Hydrometallurgical solutions are complex solutions with a large number of possible combinations of cations and anions (Krumgalz *et al.* 1995). This complexity makes solution density modeling necessary as experimental measurement of densities for multi-component solutions at different temperatures and different concentrations is too difficult an exercise to accomplish (Theliander *et al.* 1989).

The development of density models has been based on empirically correlating electrolyte physical properties and their compositions. This involves modeling partial molar volumes of the solvent and solute as a function of temperature and the respective experimental density. Since volume is a function of temperature and concentration, an understanding of the physical and chemical properties such as temperature, volume, pressure, concentration variations, and ionic strength on how they affect total electrolyte volume is very important in this modeling exercise.

This research was executed by combining the two modeling approaches (empirical and theoretical) for the development of a more practical and flexible model capable of predicting single and mixed electrolyte densities. This was done by generating mathematical equations based on theory and then empirically correlating the equations to experimentally measured data, thus generating constants for use in the developed model as done by Lam and co-workers, (Lam *et al.* 2008).

The two main approaches to developing models are: (i) theoretical modeling, and (ii) empirical modeling.

Theoretical modeling is based on an understanding of the underlying physics and chemistry affecting physical parameters such as ionic radii. These principles are used to derive mathematical relationships that best describe properties that need to be modeled such as volume. The derived equations are tested against experimental data. A number of scientific disciplines have applied theory to describe behavior of its parameters such as in milling of ores, (Li *et al.* 1999). Deviations from experimental data are minimized by adjusting the parameters

of the model, or by modifying the mathematical equations until acceptable correspondence are obtained.

Empirical modeling is based on fitting experimental data to a mathematical equation deduced from theoretical understanding of physical and thermodynamic properties that describe a specific property such as volume. This involves defining a mathematical equation with constants, and fitting it against experimental data to generate the constants. An example of the fitting exercise would involve using the least square method where error between model and experimental data is minimized by varying the parameters in the mathematical equation. If the fit is not good, modifications to the model equations are done with the fitting repeated and, if results are good, a model subject to validation will have been produced.

In this research project combining both approaches was done. Theoretical understanding on density volume and mass was used to deduce mathematical equations that best model ionic volumes in water. These mathematical equations were used to empirically fit experimental data to model with generation of parameters that would best model the density of any solution defined by a combination of ionic species involved in the fitting exercise.

A noteworthy observation is that electrolyte density modeling has been done initially on the premise and assumption that, because compounds dissolve in solution, no dissociation takes place. Subsequent developments on the models are based on the assumption that complete dissociation of a compound takes place to its building ionic (cation/anion) species. The latter is a more realistic assumption resulting in observed pairs of models from compound to ionic based models. A pair of models will be defined as a compound based model and its subsequent ionic based model. Reviewing models in literature, a grouping system based on mixing rules and concentration units applied in the model development. Four pairs of models were proposed: (i) equivalent concentration, (ii) linear mixing rule based on mole fractions; (iii) nonlinear mixing rule, and (iv) linear mixing rule based on mass fractions. (Full explanations of model pairs are in Chapter 2.2)

Note that the equivalent concentration group contains only one model. The Dixon model in the equivalent concentration group was chosen to show a simple model and to date no literature has

shown that it has been developed further to account for mixed electrolyte systems. For the purposes of this project, the forth group containing the Laliberte and Cooper model (Laliberte *et al.* 2004), which is based on compounds dissolved in solution will be development to model electrolyte densities accounting for ionic species dissolved in water.

Figure 1 shows the pairs of models noted above and locates this research project within the existing body of work on the topic.

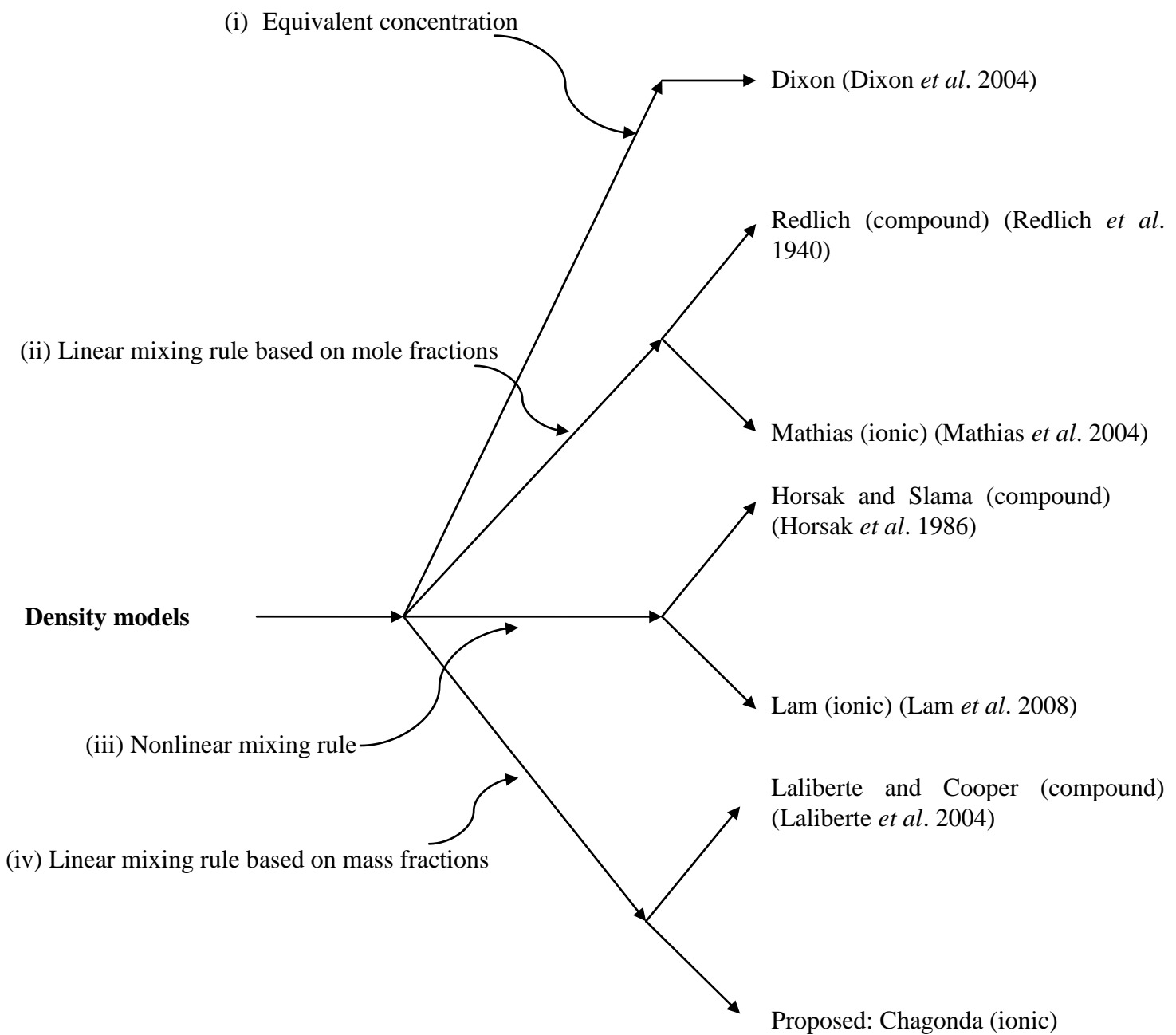


Figure 1: Tree diagram of density model pairs for compound and ionic models

The developed and extended Laliberte and Cooper model at ionic level (i.e. the proposed model) is expected to predict mixed electrolyte densities more accurately. It will therefore be easier to apply as mass fractions are simple to calculate due to existing and improved analytical instrumentation for concentration measurements.

## 2.2 DENSITY MODELS IN LITERATURE

The following section describes in detail the pairs of models illustrated in Figure 1.

### 2.2.1 EQUIVALENT CONCENTRATION MODEL

Equivalent concentration model were developed on the assumption that density of an electrolyte is equivalent to concentration of dissolved salts and the lixivants used in the dissolution process. An example is a simple model developed by Dixon (Dixon *et al* 2004). This is based on mass flow rates of water and the dissolved salts as shown in Equation 1:

$$\rho_{solution}(T) = \rho_{H_2O}(T) \left[ 1 + \alpha \left( \frac{\sum m_{solute}}{m_{H_2O}} \right) + \beta \left( \frac{\sum m_{solute}}{m_{H_2O}} \right)^2 \right] \quad \text{Equation 1}$$

where  $m$  represents mass flow rate. Water density is estimated from a temperature-density correlation such as the Kell equation (Kell *et al.* 1975). Using a reference system such as the density data for the H<sub>2</sub>SO<sub>4</sub>-H<sub>2</sub>O system, the two linear coefficients  $\alpha$  and  $\beta$  were generated:

$$\rho_{solution}(T) = \rho_{H_2O}(T) \left[ 1 + 0.6447 \left( \frac{\sum m_{solute}}{m_{H_2O}} \right) - 0.3016 \left( \frac{\sum m_{solute}}{m_{H_2O}} \right)^2 \right] \quad \text{Equation 2}$$

Equation 2 is used to estimate the solution density for metal sulfate solutions at temperature (T).

The above equations shows that the equivalent concentration model approach has capacity to model only a single media system which is a limiting factor when modeling mixed electrolyte

solutions such as in pregnant leach solutions from leaching processes were the composition of an electrolyte will consists of a variety of cations and anions in solution.

### 2.2.2 LINEAR MIXING RULE BASED ON MOLE FRACTION MODELS

Linear mixing rule models were developed on the assumption that total electrolyte volume is a sum of the dissolved ionic species and water molecules volumes without taking into account the effects of cationic/anionic species to water affecting their volume contributions. In this modeling approach, water volume is predicted as a function of water density to temperature correlation such as Kell's correlation (Kell *et al.* 1975).

Redlich and Meyer developed a model at compound level and this was further developed to ionic level by Mathias (Mathias *et al.* 2004) and Clarke (Redlich *et al.* 1940). These models are based on the linear mixing rule with concentrations calculated on mole fractions.

Total solution volume of an electrolyte is modeled as a sum function of dissolved electrolyte and water molecules. The apparent molal volume of a strong electrolyte and its concentration was defined by Masson through the empirical Equation 3:

$$V = V_w x_w + V_{elec} x_{elec} \quad \text{Equation 3}$$

where  $V$  is the molar volume of electrolyte ;  $V_w$  and  $x_w$  are the molar water volume and its concentration; and  $V_{elec}$  and  $x_{elec}$  are the electrolyte apparent molar volume and its concentration respectively.

Since  $V_{elec}$  is not the true partial molar volume of electrolyte, it has been observed that convergence of true electrolyte partial molar volume and its electrolyte apparent molar volume occurs at infinite dilution, thus the electrolyte partial molar volume has been seen to vary with the square root of its concentration as follows (Mathias *et al.* 2004):

$$V_{elec} = V_{elec}^{inf} + C_1 \sqrt{x_{elec}} \quad \text{Equation 4}$$

where  $V_{elec}$  is the electrolyte apparent molar volume;  $x_{elec}$  is its concentration in molality; and  $V_{elec}^{inf}$  is the true electrolyte partial molar volume at infinite dilution.

Redlich and Meyer further suggested extending Equation 4 as follows:

$$V_{elec} = V_{elec}^{inf} + C_1 \sqrt{x_{elec}} + C_2 x_{elec} \quad \text{Equation 5}$$

with constants  $C_1$  and  $C_2$  dependent on temperature. The concentration units used was molality – which was not compatible with higher concentrations. Therefore mole fractions were introduced for the fitting exercise.

The above equations were fitted to experimental data on molar volumes of single electrolyte solutions. The generated constants  $C_1$  and  $C_2$  were used for multi-electrolyte solution density predictions.

The Redlich and Meyer model provided an accurate correlation but did not reach the correct limit at high electrolyte concentrations due to molality units used. To overcome the concentration problem Clarke's extended Equation 5 to give Equation 6:

$$V_{elec} = V_{elec}^{inf} + V_{elec}^1 \frac{\sqrt{x_{elec}}}{1 + \sqrt{x_{elec}}} \quad \text{Equation 6}$$

where  $V_{elec}^1$  is an empirical constant related to the crystalline salt or pure liquid such as nitric acid.

Mathias then extended Clarke's model (Equation 6) to account for ionic species in water, where the parameters  $V_{elec}^{inf}$  and  $V_{elec}^1$  were defined as cation and anion pair apparent volumes respectively. This defined the total partial molar volume of electrolyte as contributions of the individual ions in the solution. This development was expected to improve the predictive capability of the model, but it has been observed to limit its predictive capabilities because the concentration is defined as that of the compound rather than of the discrete cations and anions.

To counter this limitation, modifications to Equation 6 were done. This resulted in defining of parameters independent of temperature so that they would be references for volumetric properties for the respective cation and anion in solution.

Parameters defined were (i) the pure molar volume of an ion at 25 °C ( $V_j^0$ ) and (ii) the infinite dilution partial molar volume of an ion ( $V_j^{\text{inf}}$ ). This resulted in defining  $V_{elec}^{\text{inf}}$  as a sum of the dissolved salt discrete ions as follows:

$$V_{elec}^{\text{inf}} = \sum_j x_j^{\text{ion}} V_j^{\text{inf}} + \sum_j \sum_k x_j^{\text{ion}} x_k^{\text{ion}} B_{jk} \quad \text{Equation 7}$$

where  $x_j^{\text{ion}}$  is the mole fraction of ion  $j$  on a water free basis; and  $B_{jk}$  is a binary term such that the cation and anion infinite partial molar volumes are defined as follows:

$$V_{cation}^{\text{inf}} = V_{cation}^0 - 0.02 |z_{cation}| \quad \text{Equation 8}$$

$$V_{anion}^{\text{inf}} = V_{anion}^0 + 0.01(2 - |z_{anion}|) \quad \text{Equation 9}$$

where  $V_{cation}^{\text{inf}}$ ,  $V_{anion}^{\text{inf}}$  are partial molar volumes for cations and anions at infinity dilution, and  $z_{cation}$ ,  $z_{anion}$  are the charges on the respective ionic species (Mathias *et al.* 2004).

Applying the density, mass and volume relationship, Equations 3, 7, 8 and 9 are fitted to single electrolyte density data to estimate  $V_j^{\text{inf}}$  and  $V_j^0$  parameters which are then used to model multi-component electrolyte solution densities. The model allows the possibility of binary parameters between pairs of like ions which are only used if a highly accurate multi-component correlation is required. Though useful, this modeling proved to be complicated in application; thus a simpler model was required.

### 2.2.3 NON LINEAR MIXING RULE MODELS

Nonlinear mixing rule models were developed on the assumption that total electrolyte volume is a sum of the dissolved ionic species and water molecule volume, taking into consideration the effects of cationic/anionic interactions to the water molecules to their volume contributions. In this modeling approach, parameter estimation is done for all electrolyte constituencies including dissolved cations, anions and water molecules.

Horsak and Slama (Horsak *et al.* 1986) and Lam and co-workers (Lam *et al.* 2008) developed a line of models based on the nonlinear mixing rule where the apparent molar volume of water deviates as salt concentration changes due to cation/anion and water interaction in the solution. The model developed by Horsak and Slama predicted single electrolyte densities only, while the model developed by Lam and co-workers can predict both single and multi-electrolyte solution densities.

In deriving the models, the solution was viewed as a quasi-lattice structure where water is distributed between the ionic constituencies of the dissolved salt. An equation with a parameter that accounts for change in water volume due to ionic interactions in the solution was proposed as follows:

$$V = V_s^0 x + (1-x) \left[ V_w^0 + \frac{ax}{(1+x)} \right] \quad \text{Equation 10}$$

where  $V$  is total solution molar volume;  $V_s^0$  is dissolved salt volume;  $V_w^0$  is water volume;  $a$  is the parameter accounting for deviation in water volume; and  $x$  is concentration of salt in mole fractions.

To account for cations and anions in solution complete dissociation was assumed for strong electrolytes. Equation 10 was further developed as follows:

$$V = (V_C^0 + V_A^0)x + (1-x) \left[ V_w^0 + (a_C + a_A) \frac{x}{1+x} \right] \quad \text{Equation 11}$$

where  $V_C^0$  and  $V_A^0$  are the respective cation and anion molar volumes; and  $a_C$ ,  $a_A$  are the respective cation and anion deviation parameters.

Equation 11 was then fitted to single electrolyte density data (as molar volume) for the generation of molar ionic volumes and their respective deviation parameters. This data bank was used to model single electrolyte densities according to the choice of cation and anion combinations with an ability to predict simple 1:1 aqueous solutions of electrolytes.

Building on the above equations, Lam and co-workers extended the model to predict densities of multi-electrolyte solutions. Using the density, mass and volume equation, and using equation 11, equation 12, which accounts for cations and anions in solution as a function of concentration, was developed through a number of stages and defined assumptions:

$$\rho = \frac{\sum_{i=1} x_i M_i + (1 - \sum_{i=1} x_i) M_w}{\sum_{i=1} v_i^0 x_i + v_w^0 (1 - \sum_{i=1} x_i) + \sum_{i=1} \alpha_i x_i (1 - \sum_{i=1} x_i)} \quad \text{Equation 12}$$

where  $\rho$  is the total electrolyte density;  $M_i$  is molar mass of ionic species  $i$ ;  $M_w$  is the molar mass of dissolved salt,  $x_i$  is molar fraction of ionic species  $i$ ;  $v_i^0$  is the partial molar volume of ionic species  $i$ ; and  $\alpha_i$  is the deviation parameter respective of the ionic species. In this equation the numerator calculates the solution mass according to mass fractions and the respective molar masses of the ions in solution, and the denominator calculates the total molar volume of the solution.

Equation 12 is fitted to single electrolyte density data and a data bank of  $v_i^0$  and  $\alpha_i$  is generated with an ability to predict single and multi-electrolyte solution densities.

#### 2.2.4 LINEAR MIXING RULE BASED ON MASS FRACTION MODEL

Laliberte and Cooper (Laliberte *et al.* 2004) developed a model on the linear mixing rule for partial molar volume based on mass fractions. This model predicts multi-electrolyte density as a

function of composition, temperature and coefficients derived from single electrolyte density data fitting. Total electrolyte volume is a sum of the products of salts and mass fractions with their respective apparent volumes:

$$V = w_{H_2O}v_{H_2O} + \sum_i w_i v_{app,i} \quad \text{Equation 13}$$

where  $V$  is total electrolyte volume;  $w_{H_2O}$  and  $w_i$  are mass fractions of water and dissolved salt;  $v_{H_2O}$  and  $v_{app,i}$  are apparent specific volumes of water and dissolved salt respectively. Since total electrolyte mass as a function of mass fraction is one, relating the total electrolyte volume expressed in Equation 13 and total mass fraction of electrolyte, density of electrolyte is as follows:

$$\rho = \frac{1}{w_{H_2O}v_{H_2O} + \sum_i w_i v_{app,i}} \quad \text{Equation 14}$$

For the calculation of dissolved ionic species the following equation was proposed and found to adequately represent all electrolytes studied:

$$v_{app,i} = \frac{w_i + c_2 + c_3 t}{(c_0 w_i + c_1) e^{(0.00000 t + c_4)^2}} \quad \text{Equation 15}$$

where  $v_{app,i}$  is the apparent molar volume for species  $i$ ;  $c_0$  to  $c_4$  are empirical constants; and  $t$  is temperature in degrees Celsius.

Using the Kell's equation, Equation 16 (Kell *et al.* 1975), water volume was calculated as an inverse of the water density. The calculation of water volume was based on the density, volume and mass relationship. From the Kell's equation, since water mass fraction is always one, calculating the inverse of Kell's density will correlate to water volume. See Chapter 4, section 4.4.

$$\rho_{H_2O} = \frac{(((((-2.805 \times 10^{-10} t + 1.055 \times 10^{-7}) t - 4.617 \times 10^{-5}) t - 0.00798) t + 16.945) t + 999.8352)}{1 + 0.01687 t} \quad \text{Equation 16}$$

Equations 14 and 15 were fitted to single electrolyte density data for the parameter estimation with  $c_0$  to  $c_4$  parameters generated for each electrolyte. The generated data bank of constants was used to predict mixed electrolyte solution densities as a function of temperature and concentration.

Due to the fact that Equation 14 and 15 models an electrolyte as a compound without dissociation to its cations and anions, modifications to these equations based on theoretical knowledge was done to account for cations and anions in solution since full dissociation was assumed. Equation 17 is derived to calculate single and mixed electrolyte densities:

$$\rho = \frac{1}{w_{H_2O}v_{H_2O} + \sum (w_{cation}v_{cation} + w_{anion}v_{anion})} \quad \text{Equation 17}$$

where  $w_{cation}$  and  $w_{anion}$  are the respective cation and anion mass fractions; and  $v_{cation}$ ,  $v_{anion}$  are the respective cation and anion molar volumes. Development of equations is discussed in Chapter 4: Theoretical development.

### 2.2.5 CONCLUSION

The development of a model that can accurately predict mixed solution densities is an ongoing process given the fact that a number of models have been developed to date. Reviewing the models developed to date, it is clear that the following are critical in density modeling: (i) the modeling of volume contributions of the dissolved ions in solution, (ii) the volume effect of the dissolved ions in solution on the water molecules in solution, and (iii) the effect of concentration and temperature to total electrolyte volume.

The answer towards these critical problems can be found in applying the different mixing rules in the modeling exercises. This is because the mixing rules will determine how the cations, anions and water molecules interact with each other and how these interactions affect their volumes. Therefore, for this research project, the linear mixing rule will be used. It will be used to extend the Laliberte and Cooper model, where an electrolyte will be modeled as a mixture of cations and anions dissolved in water.

The linear mixing rule assumes that there is no effect of dissolved ions on the volume of the water molecules, simplifying the modeling exercise. A simple water density to temperature correlation will be used to calculate water volume as it varies with temperature. Kell's equation (Equation 16) was used in this research project.

### 3 RESEARCH METHODOLOGY

#### 3.1 INTRODUCTION

The methodology for this research project consisted of the following five steps: (i) data sources and compilation; (ii) selection of data for fitting and model testing; (iii) processing of data for fitting (model development); (iv) minimization of the sum of squared errors; and (v) statistical testing for developed model.

Each of these steps is discussed below.

#### 3.2 DATA SOURCES

The sources of single and mixed electrolyte data used for the fitting and testing exercises are compilations taken from different sources listed in Appendix A.

#### 3.3 SELECTION OF DATA FOR FITTING AND MODEL TESTING

The data used in this research project can be divided into two sets: (i) data used for model development (the fitting exercise), and (ii) data used in the testing for the developed model (validation). The criterion used is discussed below:

(i) Data for model development (the fitting exercise)

A minimum number of salts were used so that each cation and anion was represented at least once, and the data had to satisfy the following conditions:

- (a) It had to be measured over at least three different temperatures since the Laliberte and Cooper equation used in the fitting exercise has temperature variableness.
- (b) It had to be within the temperature range of 0°C and 100°C since most of the hydrometallurgical processes to be modeled are within this temperature range.

- (c) It had to be within at least three concentration points for concentration variability.
- (d) It had to be measured at atmospheric pressure.
- (e) Salts of mainly base metals and common acids were used, including sulfates, chlorides, hydroxides, carbonates, nitrates, cyanides, sulfites, iodides, fluorides, nitrites, oxalates and bromides. These salts are known to completely dissociate in water and have known dissociation mechanisms (Plieth *et al* 2008).
- (f) Electrolytes such as sulfuric acid were avoided in this model development exercise as their dissociation in water is not well understood due to possible dissociations to the hydrogen, per-sulfate and the sulfate ions based on concentration and temperature.
- (ii) Data used for testing the developed model (validation)
  - (a) The data used in the testing of the developed model was for single and mixed electrolyte solutions. Correct prediction of single and mixed electrolyte solutions would render the purpose of this research project successful as applicability and implementation of the developed model to real hydrometallurgical processes would follow. Results obtained will also be compared to predictions of the Laliberte and Cooper model. This testing exercise will also be applied on solutions outside the conditions set for the fitting exercise, as this will serve to test the developed model's ability to extrapolate outside the concentration and temperature zones used in the model development exercise.
  - (b) Assuming complete dissociation for sulfuric acid were its dissociation will be assumed as to hydrogen and sulfate ions in water, the developed model will be tested of its predictive abilities against sulfuric acid experimental densities from Perry's Handbook of Chemical Engineering (Perry *et al.* 2008). This assumption will serve to determine to what extent is complete dissociation is true as a function of concentration and temperature.

### 3.4 PROCESSING OF DATA FOR FITTING (MODEL DEVELOPMENT)

This section covers the process of model development to ionic level and the expansion of the Laliberte and Cooper data base by parameter estimation of 39 salts not worked on before.

#### 3.4.1 PROCESSING DATA FOR MODEL DEVELOPMENT TO IONIC LEVEL

The fitting exercise was done in Microsoft Excel<sup>®</sup> spread sheets. The process involved encoding of the model equations (as discussed in Chapter 4: Theoretical development), and calculations were done according to the equations. The data was processed as follows:

- (i) Mass fractions for water, total cation and total anion were calculated using the mass percentage concentration and ionic and total compound molar masses for the dissolved salt in the electrolyte.
- (ii) For salts with cations or anions with stoichiometric values which are more than 1, single ionic mass fractions were calculated by dividing the total mass ionic mass fraction with its respective stoichiometric value.
- (iii) Using the following extended equation, cation and anion apparent specific volume in m<sup>3</sup> were calculated separately with initial guesses of c<sub>0</sub> to c<sub>4</sub> estimated for all electrolytes as 0.1, 1250, 0.1, 0.0025 and 1:

$$v_{cation/anion} = \frac{\frac{w_i}{n} + c_2 + c_3 t}{(c_0 \frac{w_i}{n} + c_1) e^{(0.00000(t+c_4)^2)}} \quad \text{Equation 18}$$

where  $n$  is the stoichiometric coefficient for the respective ion in its compound form before dissociation; and  $w_i$  is the total mass fraction for the ion. Each electrolyte cation and anion apparent specific volumes was calculated using its unique c<sub>0</sub> to c<sub>4</sub> constants so that the c<sub>0</sub> to c<sub>4</sub> produced after the fitting would enable modeling of any combination of cation and anion in any aqueous solution.

- (iv) In the same spread sheet water volume was calculated using the inverse of Kell's correlation. Kell's correlation is a prediction of water density at any temperature; thus its inverse is water volume. See Chapter 4, section 4.4.
- (v) Using the Equations 16 and 17, model density was calculated as the inverse of the sum of the products of water mass fraction and its volume, cation mass fraction and its apparent volume, and anion mass fraction and its apparent volume:
- (vi) The squared error was calculated by squaring the difference between experimental density and model density. By summing the squared errors, the sum of squared errors (SSE) was calculated in Microsoft Excel® spread sheets.

#### *3.4.2 PROCESSING DATA FOR EXPANSION OF LALIBERTE AND COOPER DATA BASE*

The fitting was done in Microsoft Excel® spread sheets where single electrolyte density data was fitted to Equations 14 and 15 for the estimation of  $c_0$  to  $c_4$  parameters. The data was processed as follows:

- (i) Mass fractions for water and dissolved salt were calculated using the mass percentage concentration.
- (ii) Using Equation 15, dissolved salt apparent specific volume in  $\text{m}^3$  was calculated separately with initial guesses of  $c_0$  to  $c_4$  estimated for all electrolytes as 0.1, 1250, 0.1, 0.0025 and 1.
- (iii) In the same spread sheet water volume was calculated using the inverse of Kell's correlation. Kell's correlation is a prediction of water density at any temperature; thus its inverse is water volume. See Chapter 4, section 4.4.
- (iv) Using Equation 14, model density was calculated based on the initial guesses in section (ii). The difference between the model and experimental density was squared, with the

sum of squared errors processed in Microsoft Excel® before the minimisation process for  $c_0$  to  $c_4$  parameter estimation is done.

### 3.5 MINIMIZATION OF THE SUM OF SQUARED ERRORS

The method of minimizing the difference between the experimental density and the model density was employed for the estimation of  $c_0$  to  $c_4$  terms. The minimization was done by aid of Solver® in Microsoft Excel® spread sheet, a nonlinear least squares method. The minimization process for the model development to ionic level and expansion of the Laliberte and Cooper data base were done as follows:

$$\min \sum_{i=0}^n \sum_{j=0}^m (measured_{ij} - model_{ij})^2 \quad \text{Equation 19}$$

By minimizing the error a data base of  $c_0$  to  $c_4$  terms unique to each ionic species was generated with capabilities to predict single and mixed electrolyte densities.

### 3.6 STATISTICAL TESTING FOR DEVELOPED MODEL

In this section statistical testing methods employed in the developed model are discussed. This will also cover a section on how the Microsoft Excel® spreadsheet was prepared for testing the model on mixed electrolyte solutions.

#### 3.6.1 PROCESSING DATA FOR MODEL TESTING

Data was processed in Microsoft Excel® spread sheets as follows:

- (i) In Microsoft Excel® spread sheets mass fractions for water, total cation and total anion were calculated using their percentage mass concentration and the molar masses respectively. In the event of a common ion, calculations were done separately based on

the compound from which it was dissociating. This was done for both mixed electrolyte and single electrolyte densities.

- (ii) For salts with cations or anions with stoichiometric values greater than 1, single ionic mass fractions were calculated by dividing the total mass ionic mass fraction with its respective stoichiometric value.
- (iii) Using the generated data base for the  $c_0$  to  $c_4$  terms, specific volumes for the ions in an electrolyte were calculated with subsequent calculation of model density for the mixed electrolyte solutions. Using the statistical methods discussed below, the quality of model was investigated by comparing it with experimental densities.
- (iv) Using the generated  $c_0$  to  $c_4$  terms for the hydrogen proton and the sulfate ion, and assuming complete dissociation for sulfuric acid, sulfuric acid density was predicted and model density compared to the experimental density.

### 3.6.2 STATISTICAL METHODS

The following statistical methods were employed in analyzing the “goodness of fit” for the developed model: (i) maximum (largest) error calculations and (ii) graphical method (with  $R^2$  correlation)

#### (i) Maximum (largest) error calculation

- The error calculation is based on the difference between the experimental and model densities.
- The maximum error is considered and the percentage error calculated to determine deviation from the measured data which is a measure of goodness of fit:

$$\%error = \frac{(Experimentaldensity - Modeldensity)}{Experimentaldensity} * 100 \quad \text{Equation 20}$$

- Average percentage error is also calculated from percentage errors calculated by Equation 20.
- By plotting the model densities against the measured densities on the Cartesian-Plane”, and calculating the  $R^2$ , the goodness of fit was tested.

(ii) Graphical method

- The graphical method is done by plotting of the model density against experimental density. Using regression, a linear curve is plotted and the  $R^2$  correlation determined. This correlation will be used to measure the goodness of fit.
- $R^2$  is a regression analysis method that can be used to measure the goodness of fit of the model to the experimental densities. It is defined as the deviation of the actual value of the dependent variable to the regression line, which is the error deviation of the model to the line of best fit. In Microsoft Excel<sup>®</sup>  $R^2$  was calculated automatically based on the following equation:

$$R^2 = \frac{SS_{err}}{SS_{tot}} \quad \text{Equation 21}$$

$R^2$  has values from 0 to 1 with 1 being the best fit a curve can have.

### 3.7 CONCLUSION

The least squares method was chosen to minimize the error between model and experimental densities for the fitting exercise. This method was motivated by the fact that the linear mixing rule was assumed for the modeling of the volumetric properties of the electrolyte, implying that the volume contribution of cations, anions and water molecules in the solution are independent of each other, and merely a function of temperature and concentration.

In this research project validation is based on how well the extended model fits the experimental densities. This was checked by calculating the error and how well the model and experimental densities correlate on the Cartesian-Plane.

## 4 THEORETICAL DEVELOPMENT

### 4.1 INTRODUCTION

In this section the modeling and the associated assumptions used are discussed in detail. The following sections will show how the Laliberte and Cooper equations were extended to account for dissociation of a dissolved salt into its respective ions in an electrolyte.

### 4.2 TOTAL ELECTROLYTE VOLUME MODELLING

Electrolyte volume was modeled as total volume contributions of the water, cations and anions in solution. Assuming uniform temperature within the whole electrolyte matrix, and linear mixing within the electrolyte, the total electrolyte volume is shown in the following equation as:

$$v_m = v_{H_2O} + v_{cation} + v_{anions} \quad \text{Equation 22}$$

where  $v_m$  is the total electrolyte volume; and  $w_{H_2O}$ ,  $v_{cation}$  and  $v_{anion}$  are the respective partial apparent water, cation and anion volume contributions to the total electrolyte volume.

Since the water, cations and anions have different concentrations within the electrolyte, by including their concentrations in the equation the specific volume of the electrolyte is modeled as follows:

$$v_{ms} = v_{H_2O}w_{H_2O} + v_{cation}w_{cation} + v_{anion}w_{anion} \quad \text{Equation 23}$$

where  $v_{ms}$  becomes the total specific electrolyte volume; and  $w_{H_2O}$ ,  $w_{cation}$  and  $w_{anion}$  are the respective water, cation and anion mass fractions for the electrolyte. This implies that the total electrolyte volume is a function of apparent volumes and their respective mass fractions.

### 4.3 DENSITY FUNCTION

By principle the density, mass and volume relationship is as follows:

$$Density = \frac{Mass}{Volume} \quad \text{Equation 24}$$

Using the total electrolyte equation based on mass fraction, and the fact that the mass fraction sum of any electrolyte is unit, density is modeled as follows:

$$\rho = \frac{1}{w_{H_2O}v_{H_2O} + \sum (w_{cation}v_{cation} + w_{anion}v_{anion})} \quad \text{Equation 25}$$

where  $\rho_m$  is the total electrolyte density in  $\text{kg/m}^3$  of a solution containing water, cations and anions of known concentration as a mass fraction. The modeling of water and ionic volumes are discussed in the next two sections.

### 4.4 WATER VOLUME MODELLING

Water volume was modeled based on Kell's correlation (Equation 16), which is a correlation of water density as a function of temperature. This is a purely empirical function developed by fitting measured water densities in the temperature ranges of  $0^\circ\text{C}$  to  $150^\circ\text{C}$  to a mathematical equation by using the least squares minimization method (Kell *et al.* 1975).

Relating Equation 24 to Equation 16, for density, the mass of water mass as a mass fraction is always unit regardless of the mass of water measured. This will imply that volume of water at any temperature can be calculated by finding the inverse of the density at temperature. Thus, the inverse of Kell's correlation would calculate the water apparent volume.

## 4.5 IONIC VOLUME MODELLING

Modeling the volume for cations and anions in solution was done for each cation and anion separately to account for a single ion volume. This led to the modification of the apparent volume expression by Laliberte and Cooper, and the following equations deduced:

$$V_{cation} = \frac{\frac{w_{cation}}{n} + c_2 + c_3 t}{(c_0 \frac{w_{cation}}{n} + c_1) e^{(0.000000(t+c_4)^2)}} \quad \text{Equation 26}$$

and

$$V_{anion} = \frac{\frac{w_{anion}}{n} + c_2 + c_3 t}{(c_0 \frac{w_{anion}}{n} + c_1) e^{(0.000000(t+c_4)^2)}} \quad \text{Equation 27}$$

where  $w_{cation}$  and  $w_{anion}$  are the total mass fractions for cations and anions; and  $n$  is the stoichiometric coefficient of either the anion or cation in the electrolyte solution. For example, sodium chloride dissolved in solution would have  $n$  values of 1 for both cation and anion; and for aluminium chloride electrolyte the  $n$  values would be 1 for the aluminium cation and 3 for the chloride cation. This proposed estimation of the  $c_0$  to  $c_4$  parameters was done based on modeling apparent specific volume of a single ion in solution.

## 4.6 CONCLUSION

The equations used by Laliberte and Cooper were modified based on the linear mixing rule. This total volume was modeled as the sum of the cations, anions and water molecules in solution multiplied by their respective mass fraction contribution. For the cations and anions the

equation for volume was developed with considerations of the stoichiometric contribution of each ion from the dissolved salt. This stoichiometric contribution brought modification of the equation in such a way that the modeled volume was for one ionic species in solution, thus the total contribution determined by its population that is its measured concentration.

For water, volume was based on pure water correlation done by Kell, where water density was correlated based on temperature; thus volume was predicted as the inverse of the water density since the mass fraction is always 1.

## 5 RESULTS AND DISCUSSIONS

### 5.1 INTRODUCTION

This section presents results obtained in the parameter estimations and the results from the modeling exercises. A total of 26 single aqueous electrolytes with 4494 data points were used for the fitting of model parameters. These salts are shown in Appendix B with their respective temperature ranges in which density was measured and their respective minimum and maximum concentrations in mass fractions.

From these salts, the apparent volumes were modeled for a total of 18 cations and 12 anions. Combining these cations and anions translates to at least 216 single electrolyte solutions which can be modeled. This also implies that a solution with at most 10 anions can be easily modeled. This is desirable for complex hydrometallurgical solutions in reality.

### 5.2 ESTIMATED PARAMETERS FOR SOLUTION DENSITY MODEL FOR 39 ADDED SALTS

Table 5.1 shows the 39 salts with  $c_0$  to  $c_4$  parameter estimated. These salts had not been included in the work done by Laliberte and Cooper and are included in this research project. Calculating the volumetric parameters for these 39 salts provided a platform for comparison of the predictive ability of the developed ionic model to the Laliberte and Cooper model (See Figures 20 – 25).

Table 5.1: Values of  $c_0$  to  $c_4$  for 39 salts from Equation 14.

Dissolved salt	Apparent volumes					Temperature		Concentration	
	$c_0$	$c_1$	$c_2$	$c_3$	$c_4$	tmin °C	tmax °C	wi min	wi max
$(\text{NH}_4)_2\text{Cr}_2\text{O}_7$	24.399	204.840	0.998	-0.022	1500.442	12.00	12.00	0.01000	0.20000
$\text{NH}_4\text{Al}(\text{SO}_4)_2$	16.583	1.595	-0.028	0.001	2274.216	40.00	80.00	0.02000	0.22000
$(\text{NH}_4)_2\text{C}_2\text{O}_4$	0.671	1.517	0.446	0.003	2532.046	20.00	80.00	0.02000	0.11000
$\text{CH}_3\text{COONH}_4$	87.509	153.791	0.044	0.050	1516.573	25.00	25.00	0.01000	0.45000
$\text{H}_3\text{AsO}_4$	232.120	523.670	1.515	0.025	1507.270	15.00	15.00	0.01000	0.70000
$(\text{NH}_4)_2\text{CrO}_4$	0.867	1.304	0.652	0.002	2662.345	13.00	20.00	0.03800	0.28040
$\text{Cd}(\text{NO}_3)_2$	1674.966	4709.175	10.272	0.304	1604.100	18.00	18.00	0.02000	0.50000
$\text{Ca}(\text{OH})_2$	1.001	1.922	-0.007	0.000	1500.003	15.00	25.00	0.05000	0.15000
$\text{CaOCl}_2$	12.346	122.416	3.489	-0.224	1500.750	15.00	15.00	0.02000	0.12000
$\text{CrO}_3$	119.662	505.553	-13.957	1.037	1543.318	15.00	15.00	0.01000	0.60000
$\text{Cu}(\text{NO}_3)_2$	96.374	503.072	5.054	-0.211	1505.965	20.00	20.00	0.01000	0.25000
$\text{Co}(\text{NO}_3)_2$	-1410.133	3259.544	9.734	0.052	1664.140	25.00	80.00	0.10000	0.60000
$\text{Fe}(\text{NO}_3)_3$	117.322	621.841	5.672	-0.235	1507.349	18.00	18.00	0.01000	0.25000
HBr	161.824	527.541	1.608	0.011	1554.612	4.00	25.00	0.01000	0.65000
HF	-2355.899	4704.944	139.509	2.024	2035.344	0.00	20.00	0.05000	0.95000
$\text{H}_2\text{O}_2$	127.461	177.418	0.502	0.037	1508.031	18.00	18.00	0.01000	1.00000
$\text{H}_2\text{SiF}_6$	3562.686	20701.915	51.567	1.541	1588.669	17.50	17.50	0.01000	0.34000
$\text{Ni}(\text{NO}_3)_2$	108.729	446.944	2.831	-0.106	1506.489	20.00	20.00	0.01000	0.35000
$\text{HClO}_4$	260.312	8.036	-0.055	0.006	1475.291	15.00	25.00	0.01000	0.70000
$\text{KHCO}_3$	89.347	108.183	0.340	0.000	1506.555	0.00	100.00	0.01000	0.10000
KBr	14999.780	40131.172	235.312	19.412	1925.410	20.00	20.00	0.01000	0.40000
$\text{K}_2\text{CrO}_4$	76.603	292.249	0.568	0.001	1508.812	15.00	18.00	0.01000	0.30000
$\text{KClO}_3$	4.718	47.443	0.143	0.000	1502.059	0.00	100.00	0.01000	0.04000
$\text{K}_2\text{Cr}_2(\text{SO}_4)_4$	979.399	585.867	-12.384	2.387	2109.029	15.00	15.00	0.01000	0.50000
$\text{K}_2\text{Cr}_2\text{O}_7$	11.252	151.589	5.612	-0.260	1500.690	20.00	20.00	0.01000	0.10000
$\text{K}_2\text{SO}_3$	71.901	279.697	2.941	-0.163	1504.955	15.00	15.00	0.01000	0.26000
$\text{K}_3\text{Fe}(\text{CN})_6$	1565.202	290.114	0.185	-0.001	-464.612	65.00	85.00	0.05000	0.40000
$\text{Na}_2\text{C}_2\text{H}_3\text{O}_2$	112.373	497.867	4.378	-0.085	1506.721	20.00	20.00	0.01000	0.28000
$\text{Na}_3\text{AsO}_4$	12.372	169.851	4.127	-0.251	1500.814	17.00	17.00	0.01000	0.12000
$\text{Na}_2\text{Cr}_2\text{O}_7$	71.118	176.417	1.489	-0.064	1503.062	15.00	15.00	0.01000	0.50000
HCOONa	0.795	1.389	0.773	0.002	2689.098	25.00	25.00	0.01000	0.40000
$\text{Na}_2\text{CrO}_4$	61.627	276.472	3.392	-0.170	1504.381	18.00	18.00	0.01000	0.26000
NaS	18.813	142.029	2.999	-0.175	1501.273	18.00	18.00	0.01000	0.18000
$\text{Na}_2\text{S}_2\text{O}_3 \cdot 5\text{H}_2\text{O}$	122.214	362.842	2.192	-0.017	1506.990	19.00	19.00	0.01000	0.50000
$\text{SnCl}_4$	232.847	402.946	1.122	-0.006	1514.720	15.00	15.00	0.01000	0.70000
$\text{SnCl}_2$	255.950	473.932	1.350	-0.010	1516.263	15.00	15.00	0.01000	0.65000
$\text{ZnBr}_2$	210.096	270.293	0.306	0.005	1537.235	0.00	100.00	0.02000	0.65000
$\text{Zn}(\text{NO}_3)_2$	538.415	3810.600	31.064	-1.674	552.541	18.00	18.00	0.02000	0.50000

### 5.3 DATA BASE FOR $c_0$ TO $c_4$ TERMS GENERATED FOR IONIC SPECIES

Table 5.2 shows the data base for  $c_0$  to  $c_4$  terms unique to each cation and anion generated during the fitting process of the 26 single electrolyte solutions used above.

Table 5.2: Generated apparent volume terms for ionic species

Dissolved ion	Apparent volume terms				
	$c_0$	$c_1$	$c_2$	$c_3$	$c_4$
Al <sup>3+</sup>	1.000E-01	5.173E+03	5.653E-03	2.885E-04	1.080E+02
Ba <sup>2+</sup>	1.000E-01	2.417E+03	8.416E-02	1.331E-04	1.103E+02
Ca <sup>2+</sup>	9.994E-02	4.304E+02	6.226E-03	6.814E-05	1.177E+02
Cd <sup>2+</sup>	1.000E-01	2.508E+03	3.235E-02	1.757E-03	1.109E+02
Co <sup>2+</sup>	1.000E-01	1.155E+03	-6.823E-02	-5.108E-04	1.122E+02
Cu <sup>2+</sup>	1.000E-01	4.614E+02	-1.430E-01	6.037E-04	9.497E+01
Fe <sup>3+</sup>	1.003E-01	3.141E+02	4.565E+00	3.657E-02	2.030E+03
Fe <sup>2+</sup>	9.994E-02	1.140E+02	-4.009E-02	4.859E-05	1.171E+02
H <sup>+1</sup>	9.999E-02	3.407E+01	3.095E-01	1.640E-03	1.012E+00
K <sup>+1</sup>	1.001E-01	1.591E+03	1.013E+00	2.151E-03	6.071E+02
Li <sup>+1</sup>	1.001E-01	5.393E+02	7.833E-01	6.323E-05	1.319E+02
Mg <sup>2+</sup>	1.000E-01	1.048E+02	-5.547E-02	-5.189E-05	9.657E+01
Mn <sup>+2</sup>	1.000E-01	8.383E+02	-5.127E-04	-2.374E-05	5.078E+01
Na <sup>+1</sup>	1.013E-01	1.609E+02	1.384E-01	1.864E-03	1.353E+03
NH4 <sup>+1</sup>	1.009E-01	4.143E+03	6.053E+00	5.435E-03	-1.741E+00
Ni <sup>2+</sup>	1.000E-01	9.604E+02	-1.547E-01	1.973E-05	9.856E+01
Sr <sup>+2</sup>	1.000E-01	9.918E+02	6.763E-03	2.349E-05	1.073E+02
Zn <sup>2+</sup>	1.012E-01	1.556E+03	1.737E-01	1.197E-03	9.675E+01
SO4 <sup>-2</sup>	1.000E-01	8.735E+03	1.258E+00	3.802E-04	1.996E+02
Cl <sup>-1</sup>	1.002E-01	1.033E+04	2.621E+00	1.994E-03	9.931E-01
CN <sup>-1</sup>	1.012E-01	4.312E+03	3.794E+00	7.327E-03	1.823E+02
NO3 <sup>-1</sup>	9.972E-02	6.602E+02	1.019E+00	5.684E-03	1.353E+03
CO3 <sup>-2</sup>	9.996E-02	6.983E+02	-1.946E-01	-1.256E-04	8.028E+01
OH <sup>-1</sup>	1.005E-01	4.512E+02	-1.424E-01	-1.596E-04	2.224E+02
SO3 <sup>-2</sup>	1.000E-01	1.045E+03	5.607E-02	-1.370E-04	1.114E+02
Br <sup>-1</sup>	1.001E-01	6.509E+03	1.188E+00	1.132E-03	2.538E+01
F <sup>-1</sup>	1.000E-01	3.377E+03	2.089E-02	3.881E-04	1.050E+02
I <sup>-1</sup>	1.002E-01	4.430E+04	1.084E+01	4.222E-03	-1.058E+01
C2O4 <sup>-2</sup>	1.001E-01	5.964E+06	1.598E-02	5.860E+00	3.909E+01
NO2 <sup>-1</sup>	3.236E+00	2.168E+01	1.917E+00	1.860E-02	2.366E+03

Table 5.2 is a compilation of the volumetric parameters unique for each dissolved ion in an electrolyte. Using the modified equations for density and cationic, anionic and the Kell's correlation discussed in Section 4, any solution containing a combination of the above ions can have its total density predicted at temperature range of -30°C to over 100°C and concentrations within solubility of the electrolyte.

The prediction mechanism can be automated by transferring these parameters into a simulator such as in Cycad Process<sup>®</sup>. With this software density and volume of the slurry produced in hydrometallurgical processes can be predicted in real time as the proposed reaction mechanisms take place.

#### 5.4 DATA FITNESS FOR SINGLE ELECTROLYTES USED IN THE FITTING EXERCISE

Table 5.3 depicts the 26 single aqueous electrolytes and the error analysis done as a difference between the experimental and model densities:

$$\text{error} = \text{experimental density} - \text{model density} \quad \text{Equation 28}$$

$$\% \text{error} = \frac{(\text{Experimental density} - \text{Model density})}{\text{Experimental density}} * 100 \quad \text{Equation 29}$$

Table 5.3: Electrolytes used in the fitting exercise and error analysis

Dissolved salt	Temperature °C		Mass fractions		Largest error g/cm <sup>3</sup>	Average % error %
	lowest	highest	Wi low	Wi high		
Al <sub>2</sub> (SO <sub>4</sub> ) <sub>3</sub>	15	95	0.00972	0.39800	0.0154	0.6718
BaCl <sub>2</sub>	0	140	0.02000	0.23801	0.0157	0.0340
CaCl <sub>2</sub>	0	75	0.02000	0.34296	0.0126	0.0051
CdSO <sub>4</sub>	25	75	0.00001	0.29671	0.0164	0.1931
CoCl <sub>2</sub>	15	75	0.00131	0.27234	0.0057	0.0204
CuSO <sub>4</sub>	0	60	0.01000	0.28440	0.0042	-0.0042
FeCl <sub>3</sub>	0	30	0.01000	0.40000	0.0115	0.4070
FeSO <sub>4</sub>	15	75	0.00711	0.21091	0.0151	-0.0343
HCl	-5	100	0.01000	0.38000	0.0332	0.2684
HCN	0	15	0.15356	1.00000	0.0072	0.0446
HNO <sub>3</sub>	-10	100	0.18100	0.60000	0.0091	-0.0325
K <sub>2</sub> CO <sub>3</sub>	0	100	0.01000	0.58240	0.0109	0.0170
LiCl	5	95	0.00212	0.04890	0.0053	0.0284
MgSO <sub>4</sub>	0	125	0.00012	0.09716	0.0106	0.0423
MnCl <sub>2</sub>	15	75	0.00122	0.28179	0.0104	-0.1546
Na <sub>2</sub> SO <sub>3</sub>	19	80	0.01000	0.20000	0.0085	-0.0774
NaF	0	98.67	0.00041	0.01812	0.0066	0.2287
NaI	10	92.23	0.27318	0.75037	0.0116	0.0043
NaOH	0	120	0.01000	0.70000	0.0241	0.1155
(NH <sub>4</sub> ) <sub>2</sub> SO <sub>4</sub>	0	100	0.01000	0.50000	0.0204	0.5692
NiCl <sub>2</sub>	15	75	0.00117	0.27263	0.0054	0.0108
SrCl <sub>2</sub>	15	98.81	0.00786	0.24062	0.0123	0.0543
ZnCl <sub>2</sub>	0	100	0.02000	0.50000	0.0174	0.1466
ZnBr <sub>2</sub>	0	100	0.02000	0.65000	0.0093	0.1631
(NH <sub>4</sub> ) <sub>2</sub> C <sub>2</sub> O <sub>4</sub>	20	80	0.02000	0.11500	0.0006	-0.2966
KNO <sub>2</sub>	20	80	0.05000	0.75000	0.0036	-0.0207

From the largest error calculation for the 26 salts used in the fitting exercise the following may be observed: (i) the fitting exercise was a success as errors less than 1% magnitude were recorded, (ii) since largest errors are positive, this implies that the model density is slightly less than the experimental density. This may be explained by the fact that the volumetric parameters generated predict total cationic and anionic volumes as slightly larger than the actual volume,

which can be directly attributed to the assumption used, that is the linear mixing rule applied for complete dissociation of salts. The linear mixing rule might not be correct as cationic, anionic and water volumes can be affected by the complex interactions between these species within the solution. Also, since water volume is correlated to the Kell's equation, deviated water volumes might be in use in the prediction of electrolyte density, since Kell's correlation is a density and temperature relationship measured with pure water – which is different from water with dissolved salts.

## 5.5 GRAPHICAL REPRESENTATION OF SINGLE ELECTROLYTES USED IN THE FITTING EXERCISE

Of the 26 electrolytes used in the fitting exercise, the following four electrolytes are shown as graphs (Figures 2 – 5) in this section. See all the other graphs in Appendix D. Model density is plotted against experimental density with the  $R^2$  correlation determined in Excel®.

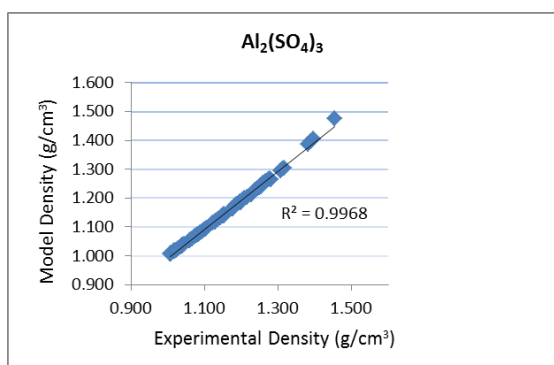


Figure 2: Plot of experimental vs. model density for  $Al_2(SO_4)_3$

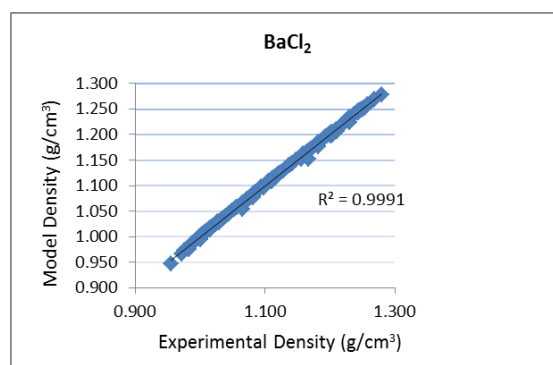


Figure 3: Plot of experimental vs. model density for  $BaCl_2$

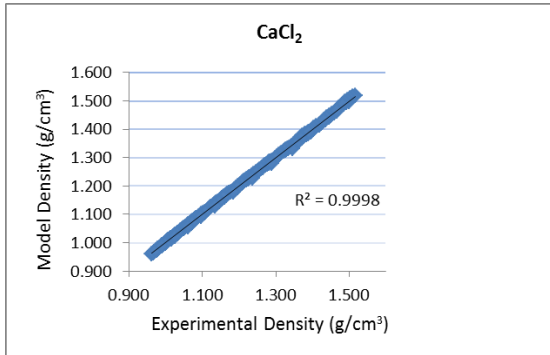


Figure 4: Plot of experimental vs. model density for CaCl<sub>2</sub>

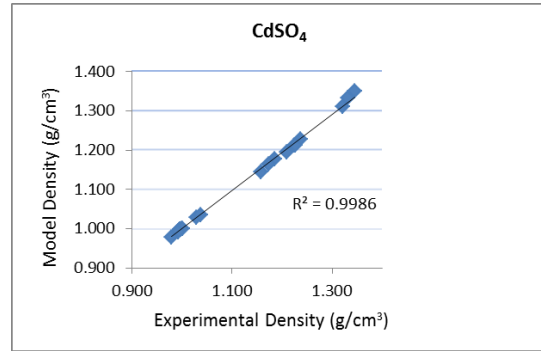


Figure 5: Plot of experimental vs. model density for CdSO<sub>4</sub>

The above graphs are plots of experimental density against extended model density. The graphs show that the fitting exercise was a success as the difference between the developed models to experimental densities is less than 1%. A correlation of over 99% on all graphs by reference to the R<sup>2</sup> value, would suggest that the generated  $c_0$  to  $c_4$  parameters may be able to predict single and mixed electrolyte densities.

## 5.6 DATA FITNESS FOR SINGLE ELECTROLYTES USED IN THE TESTING EXERCISE

The generated  $c_0$  to  $c_4$  terms were used to fit electrolyte densities for the salts not used in the fitting exercise. Table 5.4 shows the electrolytes and error analysis.

Table 5.4: Electrolytes used in the testing exercise and error analysis

Dissolved salt	Temperature °C		Mass fractions		Largest error g/cm <sup>3</sup>	Average % error %
	lowest	highest	Wi low	Wi high		
CdCl <sub>2</sub>	25	75	0.0019	0.5383	0.0096	-0.1501
CoSO <sub>4</sub>	25	75	0.0001	0.3305	0.0060	-1.2581
CuCl <sub>2</sub>	0	55	0.0100	0.4204	0.0109	-0.5190
Fe <sub>2</sub> (SO <sub>4</sub> ) <sub>3</sub>	15	25	0.0100	0.6000	0.0106	-0.7454
FeCl <sub>2</sub>	15	45	0.0032	0.2097	0.0518	0.1780
K <sub>2</sub> SO <sub>4</sub>	0	98.68	0.0005	0.1097	0.0080	0.2290
KCl	0	125	0.0001	0.2643	0.0067	-0.1243
KNO <sub>3</sub>	0	100	0.0100	0.2400	0.0023	-0.3846
KOH	0	100	0.0200	0.5946	0.1345	2.2755
Li <sub>2</sub> SO <sub>4</sub>	0	65	0.0005	0.2602	0.0299	1.2746
MgCl <sub>2</sub>	0	100	0.0004	0.3000	0.0024	-0.4195
MnSO <sub>4</sub>	0	45	0.0000	0.3640	0.0204	0.5087
Na <sub>2</sub> CO <sub>3</sub>	0	45	0.0004	0.3082	0.0002	-0.5569
Na <sub>2</sub> SO <sub>4</sub>	0	125	0.0005	0.2400	0.0110	0.0761
NaBr	15	91.95	0.0051	0.5482	0.0001	-0.7571
NaCl	0	140	0.0006	0.2603	0.0078	-0.6079
NaNO <sub>3</sub>	0	100	0.0013	0.4682	0.0023	-1.4598
NH <sub>4</sub> Cl	0	100	0.0045	0.7874	0.0257	-0.2282
NiSO <sub>4</sub>	15	60	0.0001	0.3533	0.0172	0.6651
ZnSO <sub>4</sub>	15	60	0.0017	0.3617	0.0801	2.1371
Ca(NO <sub>3</sub> ) <sub>2</sub>	6	30	0.0200	0.6800	-0.0005	-1.2047
HBr	4	25	0.0200	0.6500	0.1441	1.5584
Mg(NO <sub>3</sub> ) <sub>2</sub>	50	105	0.3086	0.6847	-0.0293	-3.1098
Co(NO <sub>3</sub> ) <sub>2</sub>	25	80	0.1000	0.6000	-0.0036	-1.7827
NH <sub>4</sub> NO <sub>3</sub>	0	95	0.0045	0.7874	0.0257	-0.2282
Cd(NO <sub>3</sub> ) <sub>2</sub>	18	85	0.0200	0.7000	0.0143	-0.2311

Table 5.4 shows that the extended model can accurately predicted single electrolyte densities. From the largest error calculated it shows that the errors are very small, implying that the model is a good fit for the experimental data. It is interesting to note that extrapolation to temperatures outside the 0°C and 100°C worked very well with examples such as NaCl and Na<sub>2</sub>SO<sub>4</sub> fitting very well at temperature of 140 °C and 125 °C respectively as shown in Table 5.4.

Using the largest errors for each electrolyte used in the testing exercise, in Excel®, the average and standard deviation was calculated and shown in Table 5.5:

Table 5.5: Largest error analysis for single electrolyte solutions

Single electrolytes				
		g/cm <sup>3</sup>	kg/m <sup>3</sup>	% error
largest error	average	0.0226	22.62	2.26
	standard deviation	0.0397	39.66	3.97

Percentage error results shown in Table 5.5 show that the model is well able to predict single electrolyte densities as the scatter of largest errors is 39.66 kg/m<sup>3</sup>, which translates to percentage errors below 4% in relation to approximated water density of 1000 kg/m<sup>3</sup>. Also take note that the largest absolute average percentage error in Table 5.4 is 3.1098% for electrolyte Mg(NO<sub>3</sub>)<sub>2</sub>, which confirms that the developed model has predictive abilities within at least 96% accuracy.

It must be noted that most of the average percentage errors are negative. This demonstrates that the model density was greater than the experimental density, and implies that the total volume predicted by the model of the electrolyte is slightly less than the actual volume. This could lead to undersized equipment; therefore correction in practice is advised. It is noteworthy that the highest deviation is out by at most 4.0% – a fairly good prediction.

Taking note of the differences in the polarity of the largest and average percentage errors, further studies with the potential to improve this model would be to use the nonlinear mixing rule as used by Lam and company (Lam *et al.* 2008) for the calculation of total volume contributions from the cations, anions and water species in a solution. Suggestions to develop this model further would be to introduce a factor that accounts for volumetric deviation to water molecules due to cation/anion and water interactions. The deviation factor will be unique to each ion in solution, and will be a function of the electrolyte temperature.

## 5.7 GRAPHICAL REPRESENTATION OF SINGLE ELECTROLYTES USED IN THE TESTING EXERCISE

For the testing exercise 26 electrolytes were used and the following four graphs (Figures 6 – 9) are some of the single electrolyte solutions tested on the developed model. See all the other graphs in Appendix E. Model density is plotted against experimental density with the  $R^2$  correlation determined in Excel®.

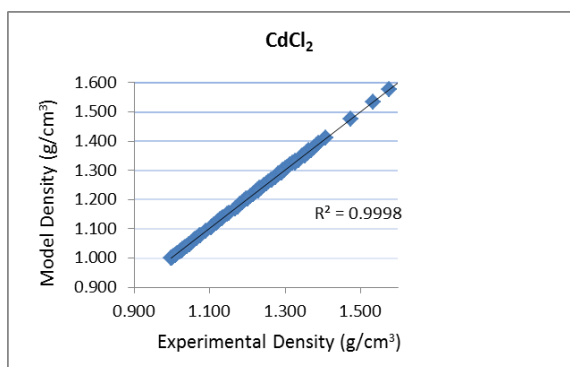


Figure 6: Plot of experimental vs. model density for CdCl<sub>2</sub>

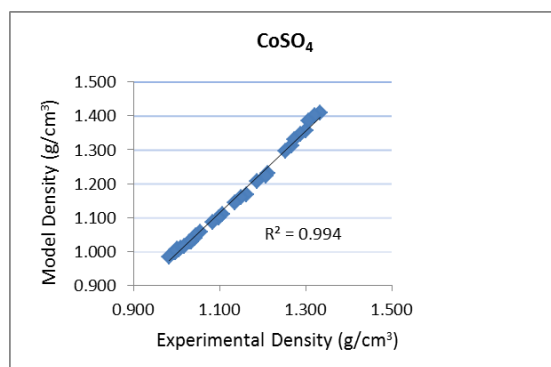


Figure 7: Plot of experimental vs. model density for CoSO<sub>4</sub>

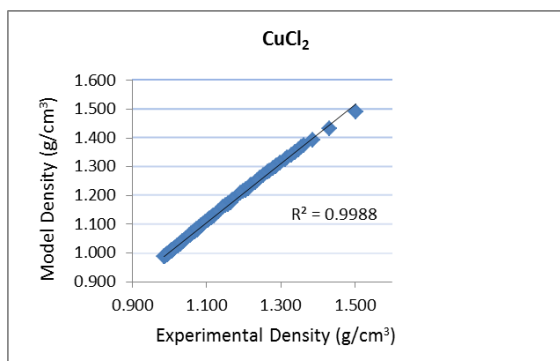


Figure 8: Plot of experimental vs. model density for CuCl<sub>2</sub>

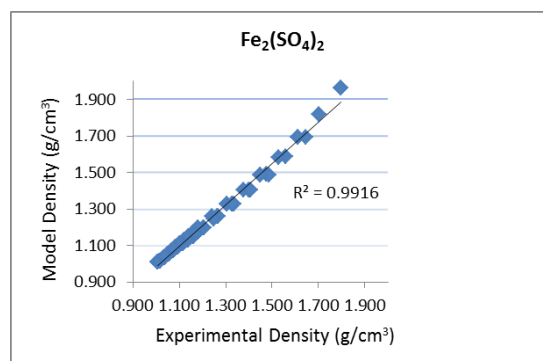


Figure 9: Plot of experimental vs. model density for Fe<sub>2</sub>(SO<sub>4</sub>)<sub>3</sub>

The graphs above are a plot of experimental density against extended model density. For all the 26 salts used in the testing exercise, the graphs demonstrate correlations of over 99% – affirming that the model fits well over different temperatures and concentrations respectively.

## 5.8 DATA AND GRAPHICAL FITNESS FOR SULFURIC ACID SOLUTIONS

Using parameters for the hydrogen ion and the sulfate anion, and assuming complete dissociation, sulfuric acid density was modeled for concentrations from 1% to 100% acid concentrations. This was done by using the volumetric parameters for the hydrogen and sulfate ions as cation and anion produces when sulfuric acid fully dissociate.

The following graphs (Figures 10 – 19) are for:

- (i) Experimental density and model density against the percentage weight at a specific temperature.
- (ii) Model density against experimental density at a specific temperature. The set of data used in this plot is up to a concentration of 30% acid in water.

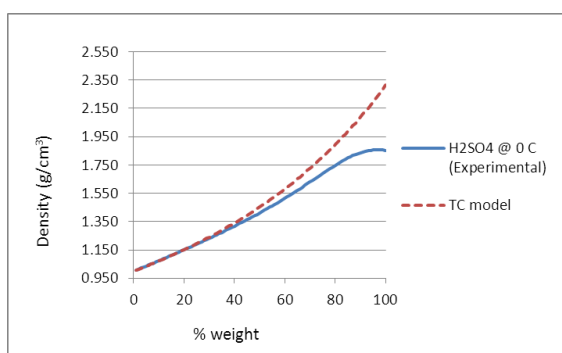


Figure 10: Plot of experimental and model density vs. % wt. for  $\text{H}_2\text{SO}_4$  at  $0^\circ\text{C}$

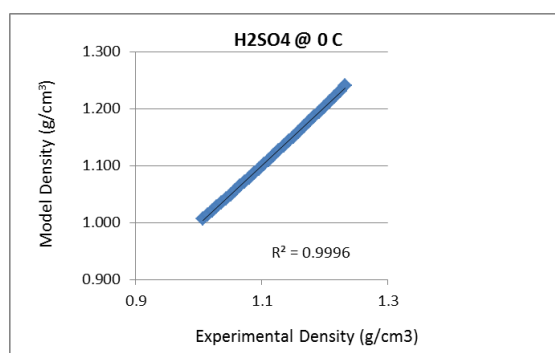


Figure 11: Plot of experimental and model density for  $\text{H}_2\text{SO}_4$  at  $0^\circ\text{C}$  up to a concentration of 30% acid in water

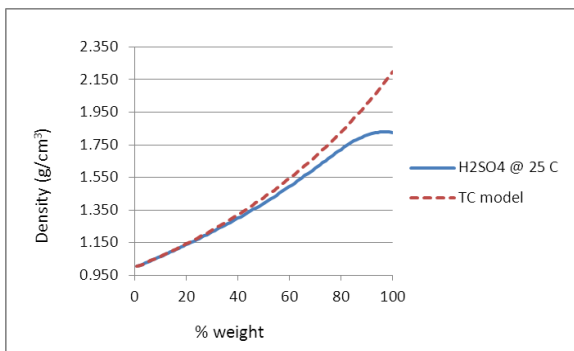


Figure 12: Plot of experimental and model density vs. % wt. for  $\text{H}_2\text{SO}_4$  at  $25^\circ\text{C}$

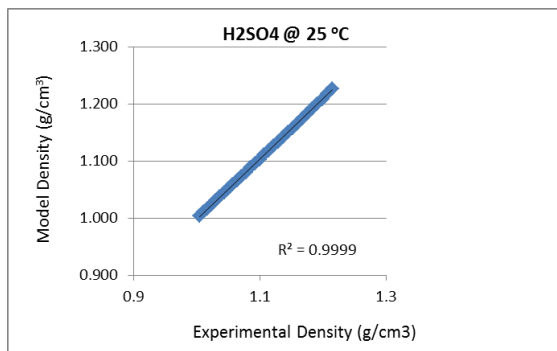


Figure 13: Plot of experimental and model density for  $\text{H}_2\text{SO}_4$  at  $25^\circ\text{C}$  up to a concentration of 30% acid in water

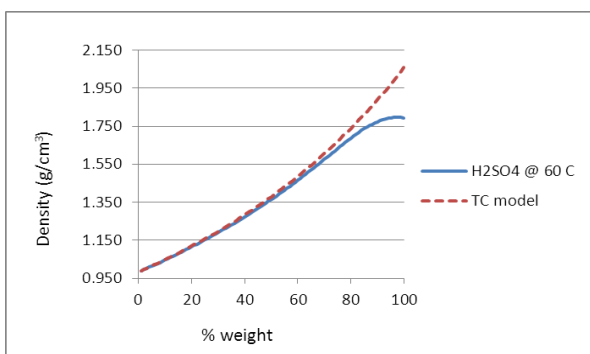


Figure 14: Plot of experimental and model density vs. % wt. for  $\text{H}_2\text{SO}_4$  at  $60^\circ\text{C}$

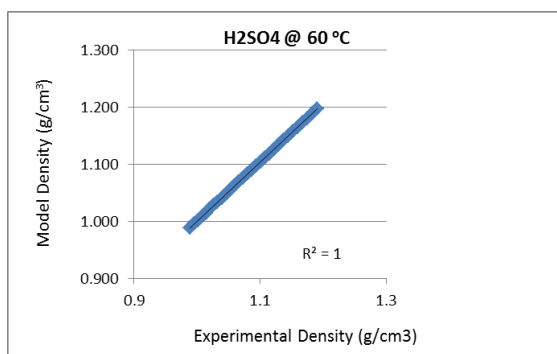


Figure 15: Plot of experimental and model density for  $\text{H}_2\text{SO}_4$  at  $60^\circ\text{C}$  up to a concentration of 30% acid in water

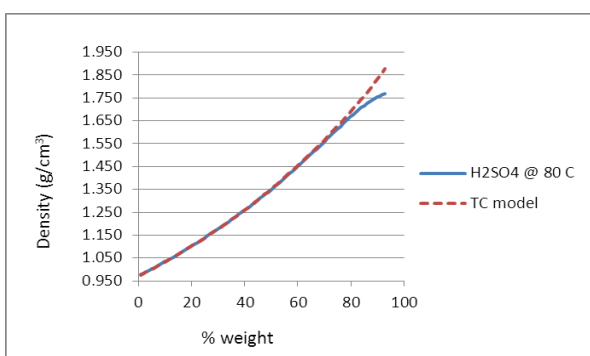


Figure 16: Plot of experimental and model density vs. % wt. for  $\text{H}_2\text{SO}_4$  at  $80^\circ\text{C}$

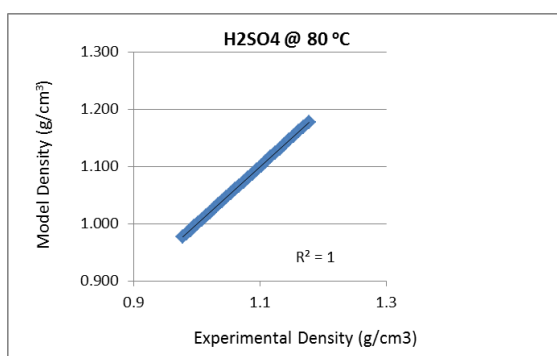


Figure 17: Plot of experimental and model density for  $\text{H}_2\text{SO}_4$  at  $80^\circ\text{C}$  up to a concentration of 30% acid in water

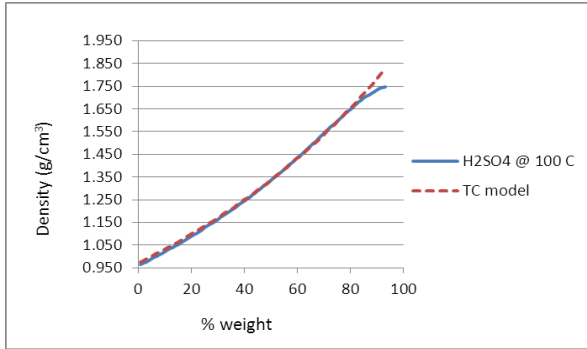


Figure 18: Plot of experimental and model density vs. % wt. for H<sub>2</sub>SO<sub>4</sub> at 100°C

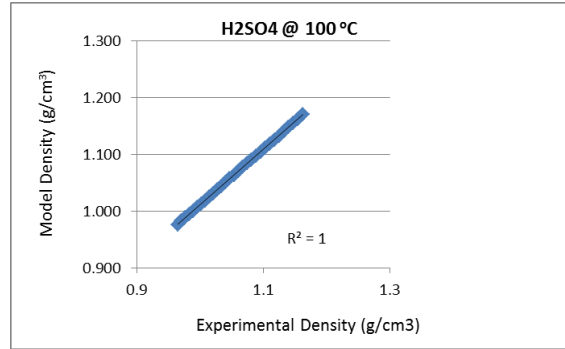


Figure 19: Plot of experimental and model density for H<sub>2</sub>SO<sub>4</sub> at 100°C up to a concentration of 30% acid in water

From the plots of experimental and model densities against percentage weight, the graphs demonstrate that the model fits well for concentrations of at least 30% acid in solution. Complete dissociation of sulfuric acid tends to increase with temperature, with an observed increase of over 80% fit at 100°C. This means that the assumption of complete dissociation within a practical concentration range for hydrometallurgy applies well for sulfuric acid, and is dependent on temperature.

Motivated by the reality that in hydrometallurgical processes sulfuric acid concentrations in mixed electrolytes rarely exceed 300 g/l even in electro-winning circuits, the 30% acid concentration limit was chosen. The 30% concentration translates to 300 g/l and according to the plot of experimental to model density plot a good correlation was achieved proving that developed model is robust.

## 5.9 DATA FITNESS FOR MIXED ELECTROLYTES SOLUTIONS

The density of 14 mixed electrolyte solutions was predicted using the generated  $c_0$  to  $c_4$  parameters for ionic species. The mixed electrolytes consisted of solutions of between 2 and 6 salts dissolved in water, and the salts contained at least 2 cations and 1 anion. Comparison for the developed model and the original Laliberte and Cooper model was done for some mixed

electrolyte solutions and, parameters for 39 dissolved salts from Table 5.2 and 59 salts from the work done before (Laliberte *et al.* 2004), were used for the Laliberte and Cooper predictions. The case study of the Hanford Waste Treatment Plant (Carter *et al.* 2007) solutions (discussed separately in the next section) was used to test and apply the developed model to a real plant scenario.

Error calculation results are shown in Table 5.6:

Table 5.6: Mixed electrolyte used for model testing and error analysis

Temperature C		Dissolved salts						Largest error	Average % error
lowest	highest								
25	25	Fe <sub>2</sub> (SO <sub>4</sub> ) <sub>3</sub>	KNO <sub>3</sub>					0.0009	-0.2260
25	25	Fe <sub>2</sub> (SO <sub>4</sub> ) <sub>3</sub>	NaNO <sub>3</sub>					0.0012	-0.4570
25	25	Fe <sub>2</sub> (SO <sub>4</sub> ) <sub>3</sub>	KBr					0.0026	0.0102
25	25	Fe <sub>2</sub> (SO <sub>4</sub> ) <sub>3</sub>	NaBr					0.0005	-0.2611
25	25	KCl	MgCl <sub>2</sub>	CaCl <sub>2</sub>				0.0014	0.0384
25	25	KCl	MgCl <sub>2</sub>	CaCl <sub>2</sub>	NaCl			0.0034	0.1209
39	59	NaCl	Na <sub>2</sub> SO <sub>4</sub>	NaOH	Na <sub>2</sub> CO <sub>3</sub>			-0.0015	-1.2559
39	59	NaCl	NaBr	NaI	KCl	KBr	KI	0.0078	-0.1441
25	175	NaCl	MgSO <sub>4</sub>					0.0204	0.5624
-30	80	H <sub>2</sub> SO <sub>4</sub>	(NH <sub>4</sub> ) <sub>2</sub> SO <sub>4</sub>					0.0147	-1.7501
-25	25	H <sub>2</sub> SO <sub>4</sub>	(NH <sub>4</sub> ) <sub>2</sub> SO <sub>4</sub>	NH <sub>4</sub> NO <sub>3</sub>				-0.0105	-2.4257
40	80	NH <sub>4</sub> Al(SO <sub>4</sub> ) <sub>2</sub>						0.0119	0.5761
65	85	K <sub>3</sub> Fe(CN) <sub>6</sub>						0.0897	3.8874
25	25	Hanford nuclear waste						0.0302	0.4045

Using the largest errors for each mixed electrolyte solution in Table 5.6 used in the testing exercise, in Excel®, the average and standard deviation was calculated and shown in Table 5.7:

Table 5.7: Largest error analysis for mixed electrolyte solutions

mixed electrolytes				
		g/cm <sup>3</sup>	kg/m <sup>3</sup>	% error
largest error	average	0.0123	12.34	1.23
	standard deviation	0.0245	24.48	2.45

Percentage error results shown in Table 5.7 show that the model is well able to predict mixed electrolyte densities as the scatter of largest errors is 2.45%, which translates to percentage errors below 3 % in relation to approximated water density of 1000 kg/m<sup>3</sup>. Also take note that

the largest absolute average percentage error for mixed electrolyte systems in Table 5.6 is 2.4257 % for the  $\text{H}_2\text{SO}_4\text{-(NH}_4)_2\text{SO}_4\text{-NH}_4\text{NO}_3$  system, confirming that the developed model has predictive abilities within at least 97% accuracy.

It is noteworthy that the model fit extrapolates well even with temperatures outside the  $0^\circ\text{C} - 100^\circ\text{C}$  range, as seen in the sulfuric acid/ammonium sulfate and the sulfuric acid/ammonium sulfate/ammonium nitrate systems where accurate predictions of densities at temperatures as low as  $-30^\circ\text{C}$  were achieved.

Tables 5.5 and 5.7 show that the developed model has the ability to reproduce the experimental densities and what the Laliberte and Cooper model predicts. Also noted in the implementation of the developed model is its flexibility in use. This flexibility is because density calculations in the developed model are done directly from ionic species concentration than the Laliberte and Cooper model where conversion of the ionic species concentrations would need to be converted to their respective dissolved compounds. Error calculations clearly show that both models predict mixed electrolyte densities very well within 99 % accuracy.

Hanford nuclear waste solutions contain electrolytes of sodium as chlorides, fluorides, phosphates, hydroxides, nitrites, nitrates, sulfates, carbonates and some mixed cationic salts such as sodium aluminate. Table 5.8 shows results of 31 electrolyte samples investigated. Qualitative and quantitative analysis for chemical identification was done; Appendix C shows the concentration results as mass fractions and the respective species. Using salt parameters developed by Laliberte and Cooper, and the developed ionic parameters, both models were tested as shown in Table 5.8 for the Hanford case study. Results obtained serve to prove that the developed model is accurate and flexible to use as direct ionic species concentrations can be used to predict electrolyte density without predicting the actual dissolved salts before.

Table 5. 8 Hanford waste models densities and error analysis results

Solution No:	experimental	developed model	Laliberte model	error	
	density (g/cm <sup>3</sup> )			developed model	Laliberte model
1	1.106	1.100	1.1019	0.0056	0.0038
2	1.096	1.098	1.0937	-0.0015	0.0025
3	1.096	1.094	1.0944	0.0019	0.0016
4	1.089	1.087	1.0868	0.0014	0.0020
5	1.091	1.089	1.0894	0.0026	0.0020
6	1.099	1.101	1.0970	-0.0019	0.0020
7	1.110	1.095	1.1120	0.0148	-0.0024
8	1.096	1.099	1.0954	-0.0035	0.0005
9	1.104	1.098	1.1020	0.0058	0.0017
10	1.102	1.093	1.0999	0.0084	0.0017
11	1.100	1.096	1.0975	0.0044	0.0030
12	1.104	1.096	1.0979	0.0081	0.0059
13	1.286	1.271	1.2719	0.0156	0.0146
14	1.262	1.272	1.2584	-0.0093	0.0038
15	1.262	1.255	1.2546	0.0063	0.0070
16	1.238	1.236	1.2311	0.0017	0.0065
17	1.245	1.240	1.2384	0.0050	0.0068
18	1.272	1.273	1.2641	-0.0006	0.0081
19	1.291	1.261	1.3133	0.0302	-0.0221
20	1.265	1.264	1.2591	0.0013	0.0060
21	1.288	1.267	1.2848	0.0209	0.0028
22	1.277	1.254	1.2769	0.0232	0.0003
23	1.276	1.263	1.2681	0.0128	0.0081
24	1.335	1.321	1.3173	0.0139	0.0175
25	1.328	1.325	1.3249	0.0028	0.0029
26	1.334	1.333	1.3349	0.0005	-0.0011
27	1.301	1.323	1.3295	-0.0214	-0.0282
28	1.312	1.342	1.3542	-0.0301	-0.0426
29	1.346	1.333	1.3308	0.0133	0.0152
30	1.368	1.354	1.3522	0.0143	0.0161
31	1.339	1.331	1.3298	0.0084	0.0093

This example is typical of a practical hydrometallurgical process. Good fittings of the developed model shown in Table 5.8 and Figure 73 gives confidence that the model developed in this research project can be applied universally.

## 5.10 GRAPHICAL REPRESENTATION OF MIXED ELECTROLYTES FITS

The following graphs (Figures 20 - 25) show plots of the developed model and the Laliberte and Cooper model against the experimental densities for mixed electrolyte solutions. The rest of graphs for mixed electrolytes are in Appendix F.

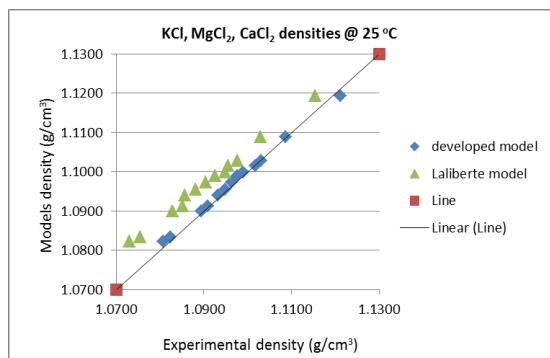


Figure 20: Plot of experimental vs. models densities for KCl, MgCl<sub>2</sub> and CaCl<sub>2</sub> at 25°C

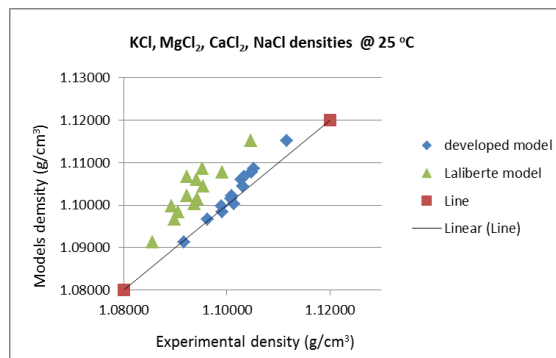


Figure 21: Plot of experimental vs. models density for KCl, MgCl<sub>2</sub>, CaCl<sub>2</sub> and NaCl at 25°C

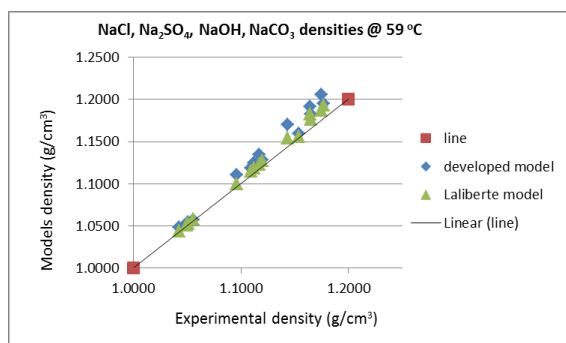


Figure 22: Plot of experimental vs. models density for NaCl, Na<sub>2</sub>SO<sub>4</sub>, NaOH and NaCO<sub>3</sub> at 59°C

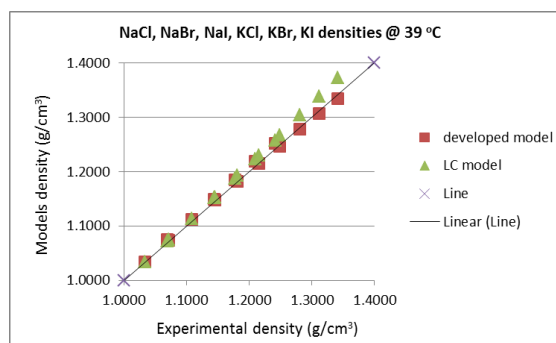


Figure 23: Plot of experimental vs. models density for NaCl, NaBr, NaI, KCl, KBr and KI at 39°C

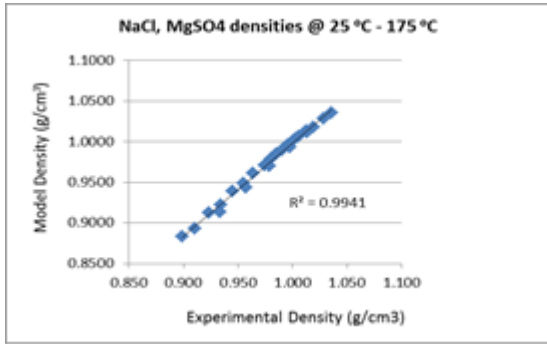


Figure 24: Plot of experimental vs. model density for NaCl and MgSO<sub>4</sub> at 25°C – 175°C

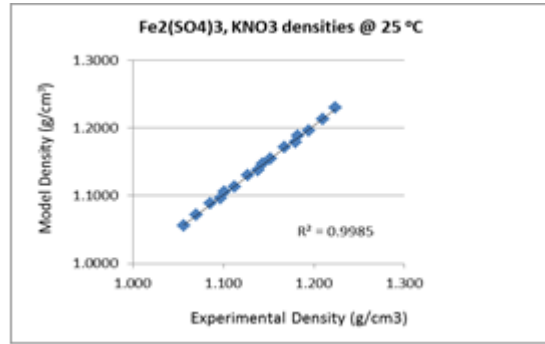


Figure 25: Plot of experimental vs. model density for Fe<sub>2</sub>(SO<sub>4</sub>)<sub>3</sub> and KNO<sub>3</sub> at 25°C

Figures 20 to 23 show plots of experimental densities against the developed and the Laliberte model densities respectively. It is clear that the developed model have an improved predicting ability as compared to the Laliberte model. Figure 24 and 25 shows other mixed electrolyte solutions with correlated sloped greater than 0.99 which is a good indication that the developed model has ability to predict experimental densities using ionic species concentrations and temperature. Other correlation graphs are in Appendix F.

## 6 CONCLUSIONS AND RECOMMENDATIONS

### 6.1 CONCLUSIONS

The following conclusions are drawn from this research project:

- A model was successfully developed to predict densities of single and mixed electrolyte solutions. The model is an extension of the Laliberte and Cooper model which models an electrolyte as a mixture of cations, anions and water molecules. The developed model has been tested and proved able to predict single and mixed electrolyte solution densities accurately. This is illustrated in Figures 20 to 25, where the developed model is compared to the Laliberte and Cooper model predictions for mixed electrolytes.
- The developed model is a more flexible method for predicting electrolyte densities as compared to the Laliberte and Cooper model. This flexibility is due to the fact that the developed model calculates using cationic and anionic concentrations as compared to the Laliberte and Cooper model where ionic species need to be converted to their dissolved salts. The developed model would be more favourable as most recent advanced qualitative and quantitative analytical instruments measure at ionic level in solution. Table 5.2 is a compilation of volumetric parameters  $c_0$  to  $c_4$  for ionic species with capability to be combined into different electrolyte solutions with correct single and mixed densities predicted.
- The complete dissociation of sulphuric acid to the hydrogen and sulfate ions is directly proportional to temperature, and inversely proportional to concentration. These relationships are observed as the fit of the modeled density to experimental density improves with increase in electrolyte temperature. The fit is also good at lower dissolved acid concentrations. In the concentration regions where the fit is poor, it is postulated that complete dissociation is not attained.

The existence of the hydrogen, sulfate and the per-sulphate ion in the electrolyte proposed.

- The combination of theoretical knowledge and empirical modelling approaches works well as a robust model was developed. The combination involved using theoretical knowledge of how density, volume and mass relate based on temperature and concentration. These relationships were used to derive mathematical equations defining model densities which were then fitted against experimental densities. The fitting exercise done using the least squares method was appropriate as fitting to over 99% was achieved.
- The expansion of the data base for the Laliberte and Cooper work was done successfully. Results of the c0 to c4 estimated parameters are shown in Table 5.1 and for purposes of comparisons done in sections 5.8 and 5.9. These results coupled with results obtained prior (Laliberte *et al.* 2004), were used against the ionic species parameters used.

## 6.2 RECOMMENDATIONS

Following the conclusions drawn from this research project, the following recommendations are proposed:

- Further development of the extended Laliberte and Cooper model developed in this research project can be achieved by use of the non-linear mixing rule. The development will be motivated by the fact that complex interactions between cations, anions and water molecules do take place within an electrolyte which should have an effect on water volume contrary to the linear mixing rule assumption that water volume is only a function of temperature. Suggestions to develop this model further are to introduce a factor that accounts for volumetric deviation to water molecules due to cation/anion interactions with water. The deviation factor will be unique to each ion in solution, and will be a function of the electrolyte concentration and temperature.

- Further testing of the developed model to recent hydrometallurgical plant processes for different systems will be useful, since many improvements have taken place for density and concentration measurement methods and instrumentations.
- Further research on sulfuric acid speciation as a function of concentration and temperature is required to determine its dissociation mechanisms. Understanding the dissociation mechanism will give an insight on how to model the acid density as the density is a dependent on concentration and temperature which defines the dissociation mechanism.

## 7 REFERENCES

- Badarayani, R., Kumar, A. and Patil, K. R. (2000). Experimental densities, speeds of sound, derived volumes and compressibilities of H<sub>2</sub>O-KCl-MgCl<sub>2</sub>-CaCl<sub>2</sub> and H<sub>2</sub>O-KCl-MgCl<sub>2</sub>-CaCl<sub>2</sub>-NaCl systems at ionic strength 3 mol/kg and at 298.15 K. (Fluid Phase Equilibria. Vol. 171, 197-206)
- Chenlo, F., Moreira, R., Pereira, G. and Vazquez, M. J. (1998). Viscosities of aqueous solutions of Fe<sub>2</sub>(SO<sub>4</sub>)<sub>3</sub> containing NaNO<sub>3</sub>, KNO<sub>3</sub>, NaBr, or KBr from 293.1 to 323.1 K. (Journal of Chemical and Engineering Data. Vol. 43, 325 – 328)
- Chun-Xi L., Sung-Bum P., Jin-Soo K. and Huen, L. (1988). A new generalized model for predicting the density of single and mixed electrolyte solutions. (Fluid Phase Equilibria. Vol. 145, 1-14)
- Dixon, D. G., Baxter, K. G. and Pavlides, A. G. (2004). Testing and modeling a novel iron control concept in a two stage ferric leach/pressure oxidation process for the Sepon Copper project. (Pressure Hydrometallurgy 2004 – 34<sup>th</sup> Annual Hydrometallurgy Meeting, 57-76)
- Fabuss, B. M., Korosi A. and Shamsul Huq, A. K. M. (1966). Density of Binary and Ternary aqueous solutions of NaCl, Na<sub>2</sub>SO<sub>4</sub> and MgSO<sub>4</sub>, of sea waters and sea water concentrates. (Journal of Chemical and Engineering Data. Vol. 11, No. 3, 325-331)
- Horsak, I. and Slama, I. (1986). Densities of aqueous electrolyte solution: A model for a data bank. (Journal of Chemical Engineering Data. Vol. 31, 434-437)
- Iulian, O., Sirbu, F. and Stoicescu, C. (2008). Density and apparent molar volume prediction in some ternary electrolyte solutions. (Revue Roumaine de Chimie. Vol. 53 No. 12, 1125-1129)
- Jubin, R. T., Marley, J. L. and Counce, R. M. (1986). Density study of Mg(NO<sub>3</sub>)<sub>2</sub>-H<sub>2</sub>O-HNO<sub>3</sub> solutions at different temperatures. (Journal of Chemical and Engineering Data. Vol. 31, No. 1, 86-88)
- Kell, G. S. (1975). Density, thermal expansivity, and compressibility of liquid water from 0 °C to 150 °C: correlations and tables for atmospheric pressure and saturation reviewed and expressed on 1968 temperature scale. (Journal of Chemical and Engineering Data. Vol. 20, No. 1, 97 – 105)
- Krumgalz, B. S., Pogorelsky, R. and Pitzer, K. S. (1995). Ion interaction approach to calculations of volumetric properties of aqueous multiple solute electrolyte solutions. (Journal of Solution Chemistry. Vol. 24, No. 10, 1025-1038)

Kumar, A. (1986). Prediction of densities of concentrated brines by Pitzer Theory. (Journal of Chemical and Engineering Data. Vol. 31, 19-20)

Laliberte, M. and Cooper, W. E. (2004). Model for calculating the density of aqueous electrolyte solutions. (Journal of Chemical and Engineering Data. Vol. 49, 1141-1151)

Lam, E. J., Alvarez, M. N., Galvez, M. E. and Alvarez, E. B. (2008). A model for calculating the density of aqueous multicomponent electrolyte solutions. (Journal of the Chilean Chemical Society. Vol. 53, No. 1)

Li, C. and Lee, H. (2000). Density calculation of electrolyte solutions with the solution osmotic pressure. (Chemical Engineering Science. Vol. 55, 655-665)

Li. X. P, Nee. A. Y. C, Wong. Y. S and Zeng. H.Q. (1999) Theoretical modelling and simulation of milling forces. (Journal of Materials Processing Technology, Vol. 89 – 90, 266 – 272).

Lobo, V. M. (1989). Handbook of Electrolyte Solutions. (Elsevier Science: New York)

Mathias, P.M. (2004). Correlation for the density of multicomponent aqueous electrolytes. (Industrial and Engineering Chemistry Research. Vol. 43, 6247-6252)

Perry, R. H. and Green, D. (2008). W. Perry's Handbook of Chemical Engineering, 8<sup>th</sup> Edition. (2-104 – 2-114).

Plieth, W. (2008). Electrochemistry for Material Science. (Dresden: Technische Universität Dresden, Chapter1, 1-26)

Redlich, O. (1940). Molal volumes of solutes. IV. (Journal of Physical Chemistry. Vol. 44, No. 5, 619-629)

Reynolds, J. G., Bernards, J. K. and Carter, R. (2007). A solution density model for Hanford Waste Treatment Plant Supernatants. (WM 2007 Conference: 25 February-1 March 2007)

Reynolds, J. G. and Carter, R. (2007). Density model for sodium hydroxide-sodium aluminate solutions. (Hydrometallurgy. Vol. 89, 233-241)

Reynolds, J. G. and Carter, R. (2008). The Laliberte-Cooper density model: Self consistency and a new method of parameterization. (Fluid Phase Equilibria. Vol. 266, 14-20)

Gephart, R.E. (2010). A short history of waste management at the Hanford Site. (Journal of Physics and Chemistry of the Earth. Vol. 35, 298-306)

Semmler, M., Luo, B. P. and Koop, T. (2006). Densities of liquid  $\text{H}^+/\text{NH}_4^+/\text{SO}_4^{2-}/\text{NO}_3^-/\text{H}_2\text{O}$  solutions at tropospheric temperatures. (Atmospheric Environment. Vol. 40, 467 – 483)

Sohnel, O., Novotny, P. and Solc, Z. (1984). Densities of aqueous solutions of 18 inorganic substances. (Journal of Chemical and Engineering Data. Vol. 29, 379-382)

Theiliander, H. and Gren, U. (1989). A simple algorithm for the estimation of the density of aqueous solutions containing two or more different salts. (Computers and Chemical Engineering. Vol. 13, No. 4/5, 419-424)

#### **APPENDIX A: SINGLE AND MIXED ELECTROLYTE DATA SOURCES**

The following is a list of data sources used for model developing and testing:

- (i) Handbook of Electrolyte Solutions (Lobo *et al.* 1989).
- (ii) Perry's Chemical Engineering Handbook, 8th Edition (Perry *et al.* 2007).
- (iii) Multi-electrolyte density data from various sources: (Badarayani *et al.* 2000), (Chenlo *et al.* 1998), (Fabuss *et al.* 1966), (Iulian *et al.* 2008), (Reynolds *et al.* 2008), (Salavera *et al.* 2004), (Semmler *et al.* 2006), (Sohnel *et al.* 1984) and (Zhang *et al.* 1997).

## APPENDIX B: SALTS USED IN THE MODEL DEVELOPMENT - FITTING EXERCISE

A total of 26 salts used in the model development and extension of the Laliberte and Cooper model to ionic level.

Dissolved salt	Temperature °C		Mass fractions	
	lowest	highest	Wi low	Wi high
Al <sub>2</sub> (SO <sub>4</sub> ) <sub>3</sub>	15	95	0.00972	0.39800
BaCl <sub>2</sub>	0	100	0.02000	0.23801
CaCl <sub>2</sub>	0	75	0.02000	0.34296
CdSO <sub>4</sub>	25	75	0.00001	0.29671
CoCl <sub>2</sub>	15	75	0.00131	0.27234
CuSO <sub>4</sub>	0	60	0.01000	0.28440
FeCl <sub>3</sub>	0	30	0.01000	0.40000
FeSO <sub>4</sub>	15	75	0.00711	0.21091
HCl	0	100	0.01000	0.30000
HCN	0	15	0.15356	1.00000
HNO <sub>3</sub>	0	100	0.18100	0.60000
K <sub>2</sub> CO <sub>3</sub>	0	100	0.01000	0.58240
LiCl	5	95	0.00212	0.04890
MgSO <sub>4</sub>	0	100	0.00012	0.09716
MnCl <sub>2</sub>	15	75	0.00122	0.28179
Na <sub>2</sub> SO <sub>3</sub>	19	80	0.01000	0.20000
NaF	0	98.67	0.00041	0.01812
NaI	10	92.23	0.27318	0.75037
NaOH	0	100	0.01000	0.70000
(NH <sub>4</sub> ) <sub>2</sub> SO <sub>4</sub>	0	100	0.01000	0.50000
NiCl <sub>2</sub>	15	75	0.00117	0.27263
SrCl <sub>2</sub>	15	98.81	0.00786	0.24062
ZnCl <sub>2</sub>	0	100	0.02000	0.50000
ZnBr <sub>2</sub>	0	100	0.02000	0.65000
(NH <sub>4</sub> ) <sub>2</sub> C <sub>2</sub> O <sub>4</sub>	20	80	0.02000	0.11500
KNO <sub>2</sub>	20	80	0.05000	0.75000

Data used satisfied conditions in Chapter 3.3 where the temperature range was required to be between 0°C and 100°C, and concentrations were required over at least three points. The generated data base for the volumetric parameters and the validations for both single and mixed electrolyte density predictions are discussed in this section.

## APPENDIX C: HANFORD ELECTROLYTE CONCENTRATIONS AS MASS FRACTIONS

Solution No:	Mass fractions for Hanford nuclear solution wastes									
	H <sub>2</sub> O	Na	Al	CO <sub>3</sub>	NO <sub>2</sub>	NO <sub>3</sub>	OH	C <sub>2</sub> O <sub>4</sub>	Cl	F
1	0.8921	0.0431	0.0083	0.0147	0.0120	0.0221	0.0062	0.0002	0.0013	0.0001
2	0.8934	0.0405	0.0023	0.0149	0.0122	0.0272	0.0061	0.0006	0.0013	0.0016
3	0.8910	0.0414	0.0023	0.0093	0.0263	0.0221	0.0061	0.0002	0.0013	0.0001
4	0.9020	0.0409	0.0024	0.0007	0.0124	0.0224	0.0157	0.0006	0.0013	0.0016
5	0.9005	0.0433	0.0024	0.0007	0.0122	0.0223	0.0170	0.0002	0.0013	0.0001
6	0.8836	0.0408	0.0023	0.0077	0.0120	0.0461	0.0060	0.0002	0.0013	0.0001
7	0.8939	0.0440	0.0157	0.0007	0.0119	0.0216	0.0102	0.0006	0.0013	0.0001
8	0.8784	0.0408	0.0023	0.0007	0.0262	0.0436	0.0060	0.0006	0.0013	0.0001
9	0.8842	0.0413	0.0075	0.0007	0.0119	0.0455	0.0059	0.0002	0.0013	0.0016
10	0.8896	0.0423	0.0092	0.0007	0.0260	0.0221	0.0070	0.0002	0.0013	0.0016
11	0.8897	0.0430	0.0063	0.0048	0.0165	0.0298	0.0076	0.0004	0.0013	0.0008
12	0.8901	0.0424	0.0063	0.0048	0.0165	0.0298	0.0076	0.0004	0.0013	0.0008
13	0.7436	0.1027	0.0197	0.0350	0.0286	0.0521	0.0148	0.0003	0.0031	0.0002
14	0.7405	0.0987	0.0057	0.0363	0.0297	0.0657	0.0147	0.0016	0.0032	0.0040
15	0.7390	0.0991	0.0056	0.0222	0.0629	0.0532	0.0145	0.0003	0.0031	0.0002
16	0.7630	0.0986	0.0058	0.0017	0.0299	0.0544	0.0378	0.0015	0.0032	0.0040
17	0.7586	0.1050	0.0059	0.0017	0.0297	0.0541	0.0413	0.0003	0.0032	0.0002
18	0.7240	0.0970	0.0054	0.0183	0.0284	0.1092	0.0142	0.0003	0.0031	0.0002
19	0.7422	0.1066	0.0380	0.0017	0.0289	0.0530	0.0248	0.0015	0.0031	0.0002
20	0.7160	0.0953	0.0054	0.0016	0.0613	0.1017	0.0140	0.0014	0.0030	0.0001
21	0.7228	0.0989	0.0180	0.0017	0.0284	0.1090	0.0141	0.0003	0.0030	0.0038
22	0.7343	0.1020	0.0222	0.0017	0.0628	0.0529	0.0169	0.0003	0.0031	0.0038
23	0.7338	0.1036	0.0152	0.0116	0.0398	0.0719	0.0182	0.0009	0.0031	0.0019
24	0.6671	0.1118	0.0063	0.0019	0.0718	0.1192	0.0165	0.0017	0.0035	0.0002
25	0.6637	0.1129	0.0064	0.0019	0.0724	0.1207	0.0166	0.0017	0.0036	0.0002
26	0.6568	0.1152	0.0065	0.0020	0.0740	0.1231	0.0169	0.0018	0.0037	0.0002
27	0.6657	0.1123	0.0063	0.0019	0.0720	0.1198	0.0165	0.0017	0.0036	0.0002
28	0.6500	0.1176	0.0066	0.0020	0.0754	0.1254	0.0173	0.0018	0.0037	0.0002
29	0.6573	0.1152	0.0065	0.0020	0.0738	0.1228	0.0169	0.0018	0.0037	0.0002
30	0.6401	0.1202	0.0068	0.0021	0.0771	0.1303	0.0176	0.0018	0.0038	0.0002
31	0.6590	0.1145	0.0065	0.0020	0.0734	0.1223	0.0168	0.0018	0.0036	0.0002

## APPENDIX D: GRAPHS FOR SINGLE ELECTROLYTE USED IN FITTING EXERCISE

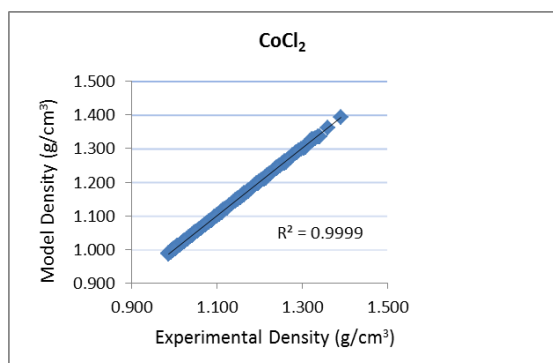


Figure 26: Plot of experimental vs. model density for  $\text{CoCl}_2$

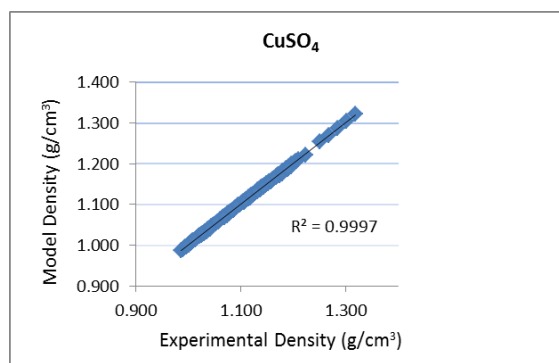


Figure 27: Plot of experimental vs. model density for  $\text{CuSO}_4$

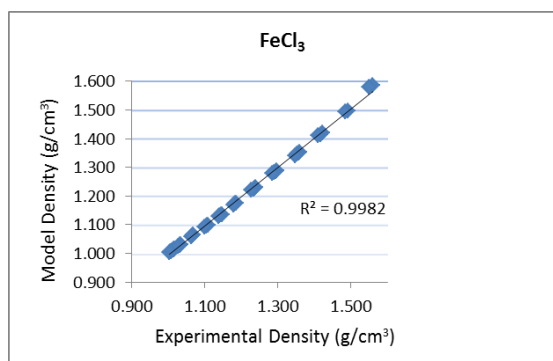


Figure 28: Plot of experimental vs. model density for  $\text{FeCl}_3$

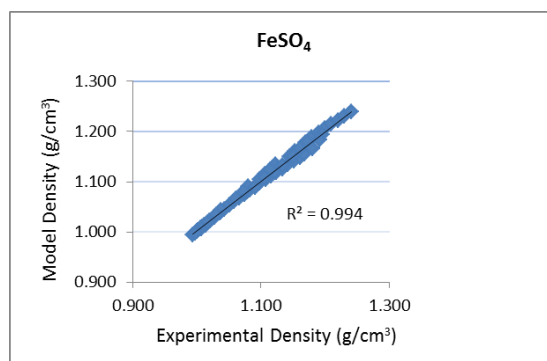


Figure 29: Plot of experimental vs. model density for  $\text{FeSO}_4$

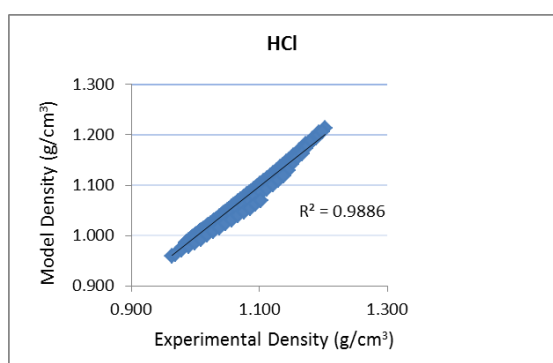


Figure 30: Plot of experimental vs. model density for  $\text{HCl}$

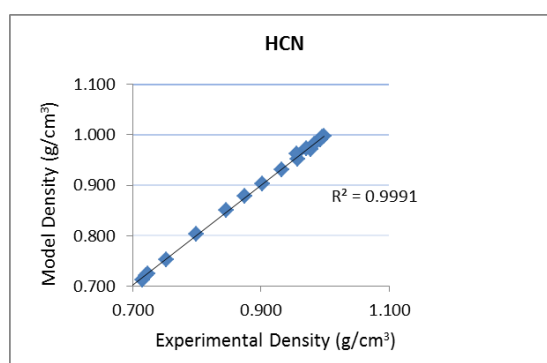


Figure 31: Plot of experimental vs. model density for  $\text{HCN}$

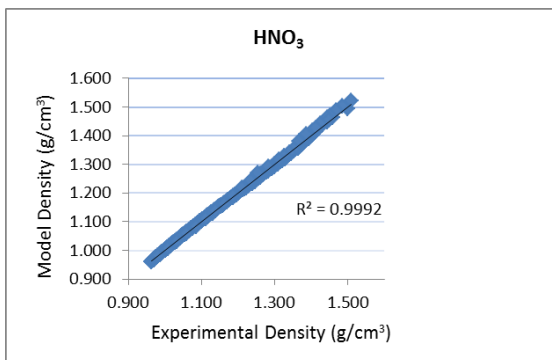


Figure 32: Plot of experimental vs. model density for HNO<sub>3</sub>

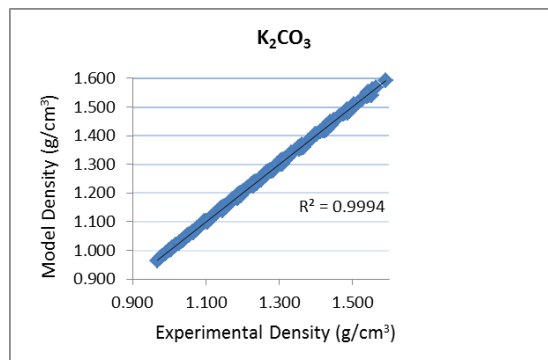


Figure 33: Plot of experimental vs. model density for K<sub>2</sub>CO<sub>3</sub>

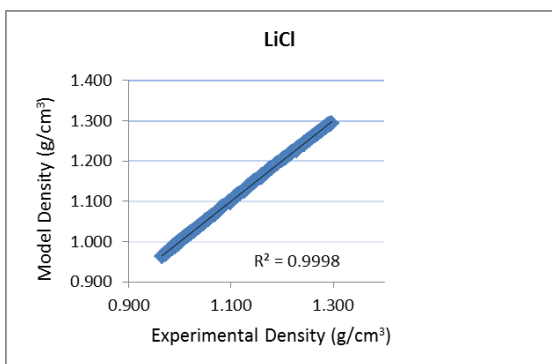


Figure 34: Plot of experimental vs. model density for LiCl

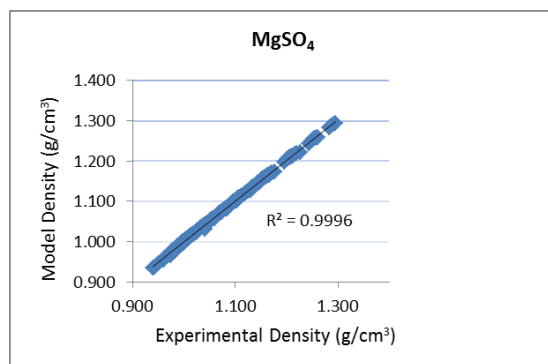


Figure 35: Plot of experimental vs. model density for MgSO<sub>4</sub>

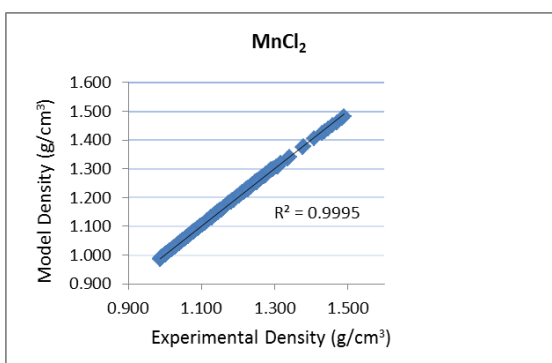


Figure 36: Plot of experimental vs. model density for MnCl<sub>2</sub>

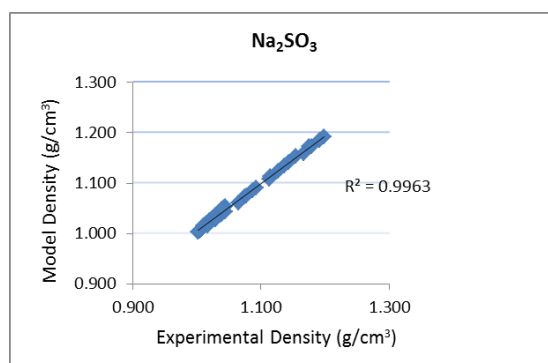


Figure 37: Plot of experimental vs. model density for NaSO<sub>3</sub>

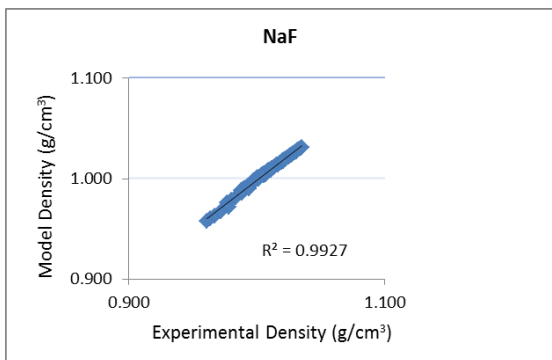


Figure 38: Plot of experimental vs. model density for NaF

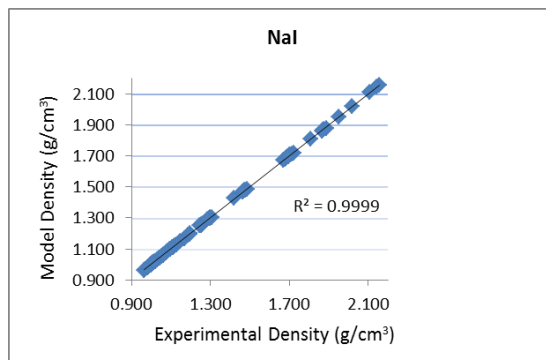


Figure 39: Plot of experimental vs. model density for NaI

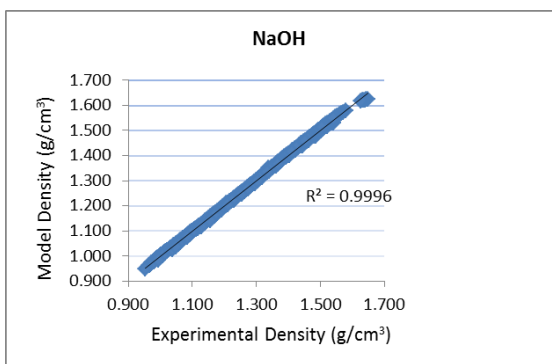


Figure 40: Plot of experimental vs. model density for NaOH

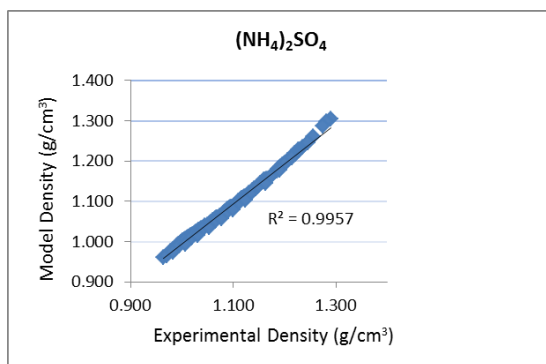


Figure 41: Plot of experimental vs. model density for (NH<sub>4</sub>)<sub>2</sub>SO<sub>4</sub>

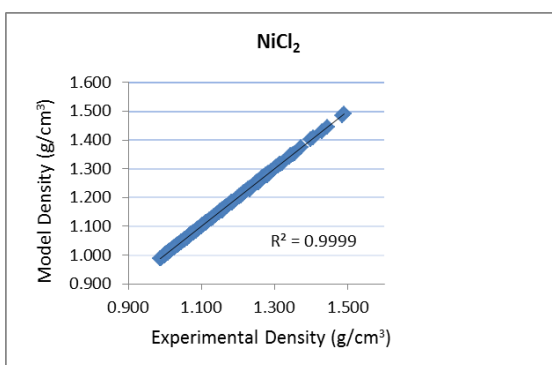


Figure 42: Plot of experimental vs. model density for NiCl<sub>2</sub>

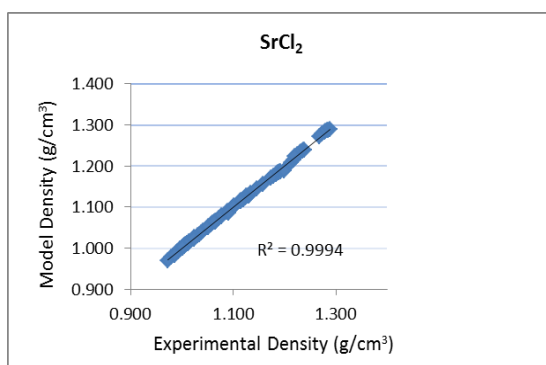


Figure 43: Plot of experimental vs. model density for SrCl<sub>2</sub>

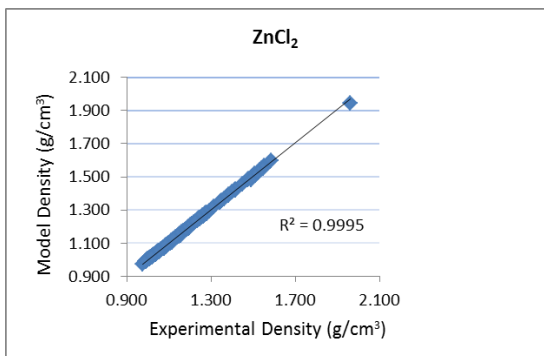


Figure 44: Plot of experimental vs. model density for ZnCl<sub>2</sub>

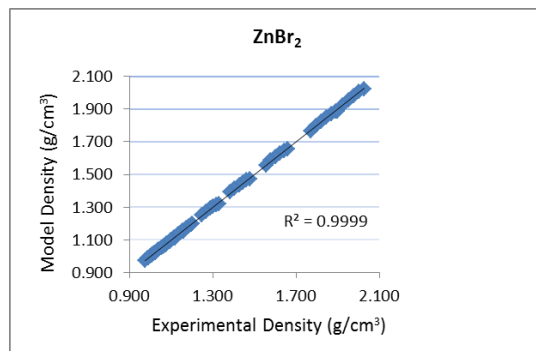


Figure 45: Plot of experimental vs. model density for ZnBr<sub>2</sub>

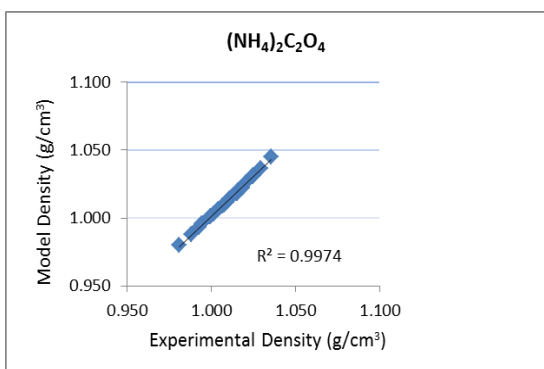


Figure 46: Plot of experimental vs. model density for (NH<sub>4</sub>)<sub>2</sub>C<sub>2</sub>O<sub>4</sub>

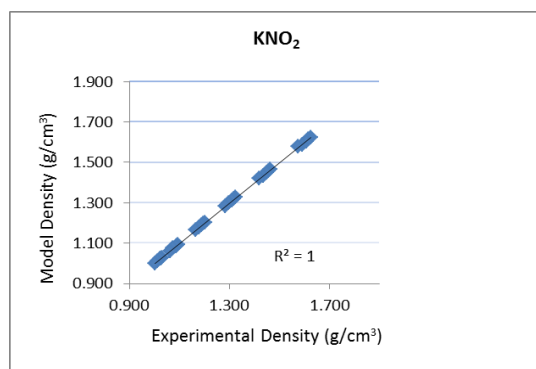


Figure 47: Plot of experimental vs. model density for KNO<sub>2</sub>

## APPENDIX E: GRAPHS FOR SINGLE ELECTROLYTE USED IN TESTING EXERCISE

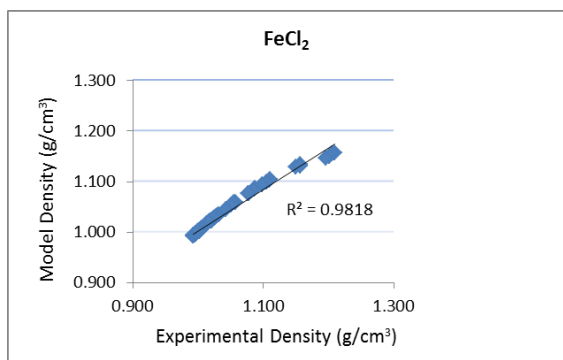


Figure 48: Plot of experimental vs. model density for FeCl<sub>2</sub>

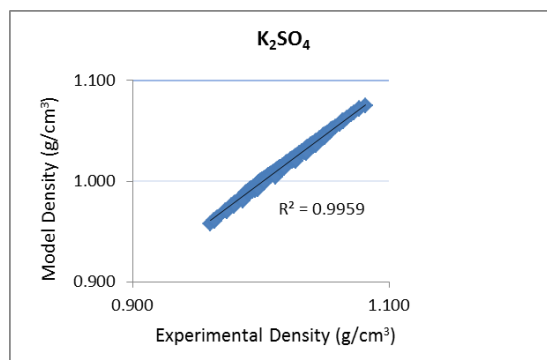


Figure 49: Plot of experimental vs. model density for K<sub>2</sub>SO<sub>4</sub>

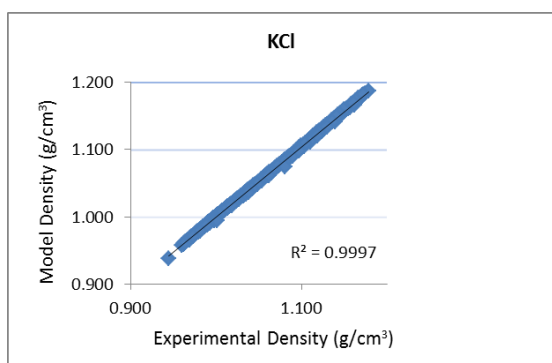


Figure 50: Plot of experimental vs. model density for KCl

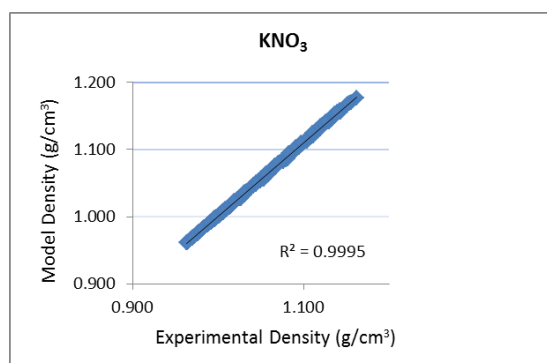


Figure 51: Plot of experimental vs. model density for KNO<sub>3</sub>

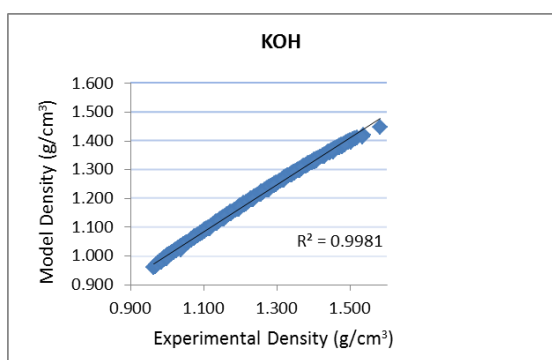


Figure 52: Plot of experimental vs. model density for KOH

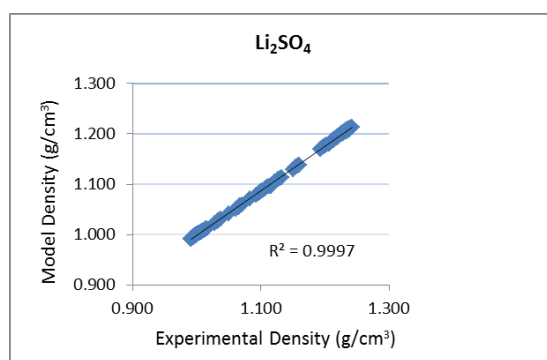


Figure 53: Plot of experimental vs. model density for Li<sub>2</sub>SO<sub>4</sub>

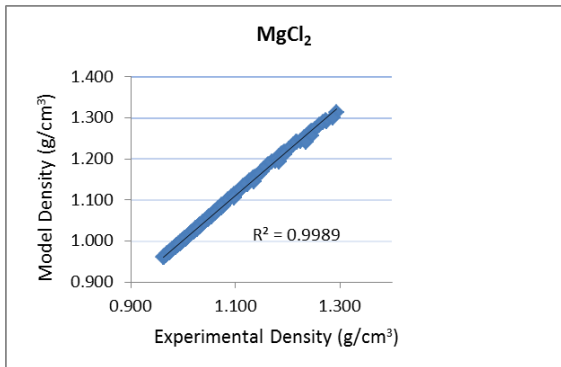


Figure 54: Plot of experimental vs. model density for  $\text{MgCl}_2$

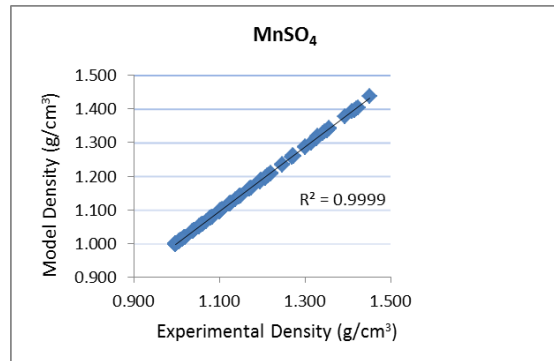


Figure 55: Plot of experimental vs. model density for  $\text{MnSO}_4$

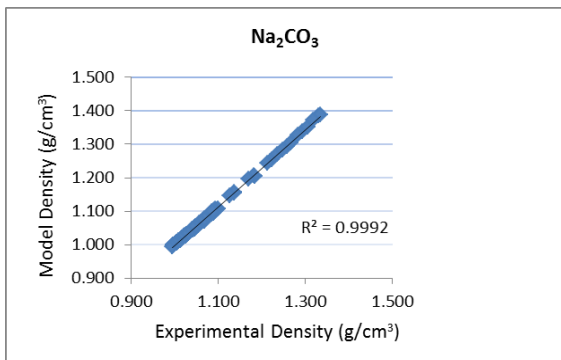


Figure 56: Plot of experimental vs. model density for  $\text{Na}_2\text{CO}_3$

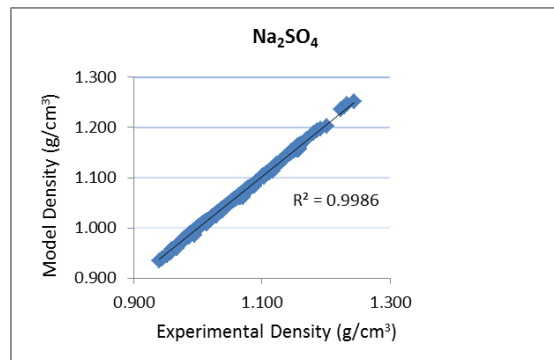


Figure 57: Plot of experimental vs. model density for  $\text{Na}_2\text{SO}_4$

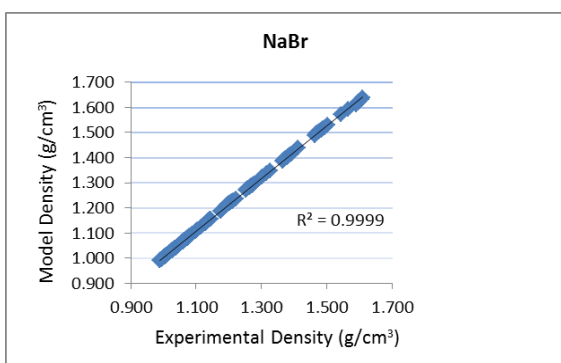


Figure 58: Plot of experimental vs. model density for  $\text{NaBr}$

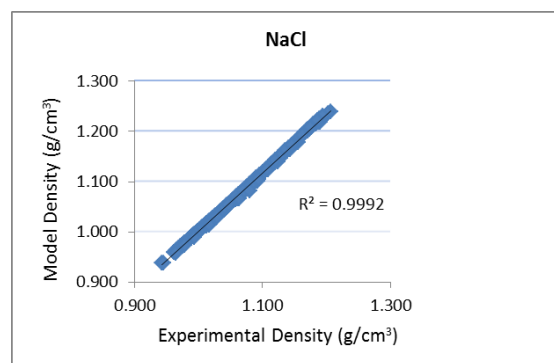


Figure 59: Plot of experimental vs. model density for  $\text{NaCl}$

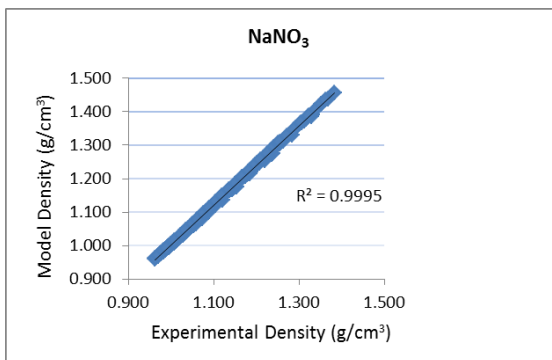


Figure 60: Plot of experimental vs. model density for NaNO<sub>3</sub>

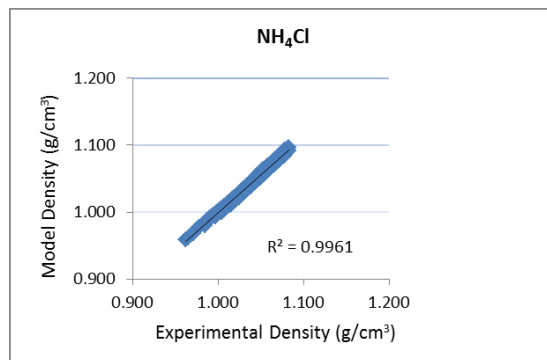


Figure 61: Plot of experimental vs. model density for NH<sub>4</sub>Cl

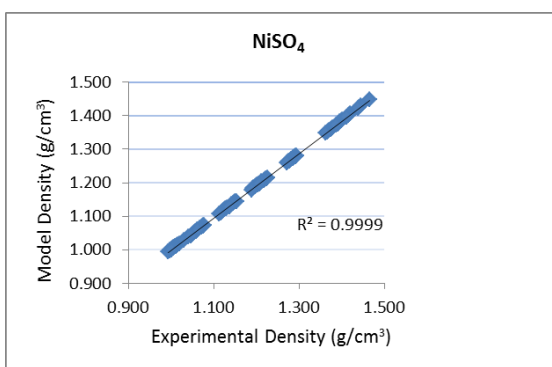


Figure 62: Plot of experimental vs. model density for NiSO<sub>4</sub>

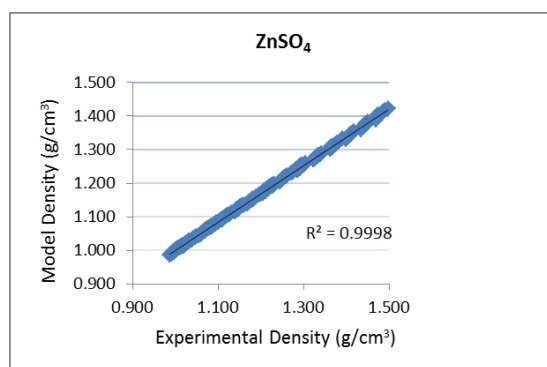


Figure 63: Plot of experimental vs. model density for ZnSO<sub>4</sub>

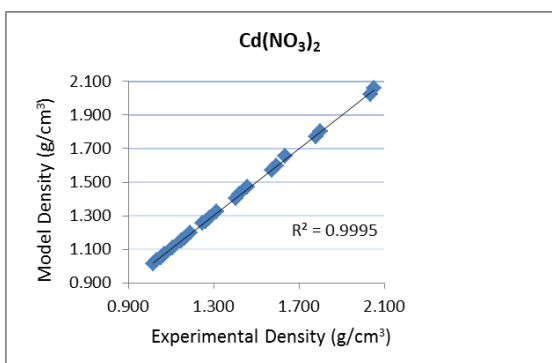


Figure 64: Plot of experimental vs. model density for Cd(NO<sub>3</sub>)<sub>2</sub>

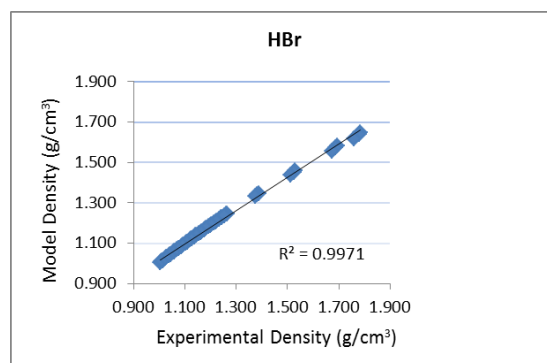


Figure 65: Plot of experimental vs. model density for HBr

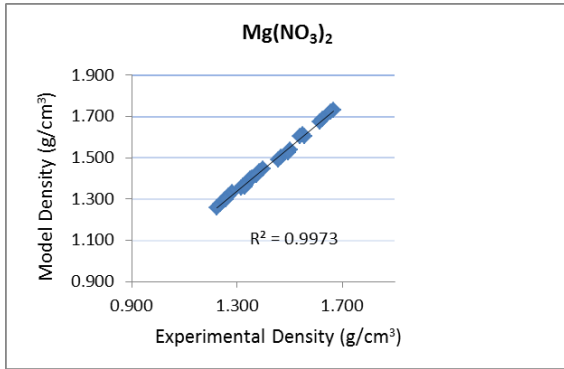


Figure 66: Plot of experimental vs. model density for  $\text{Mg}(\text{NO}_3)_2$

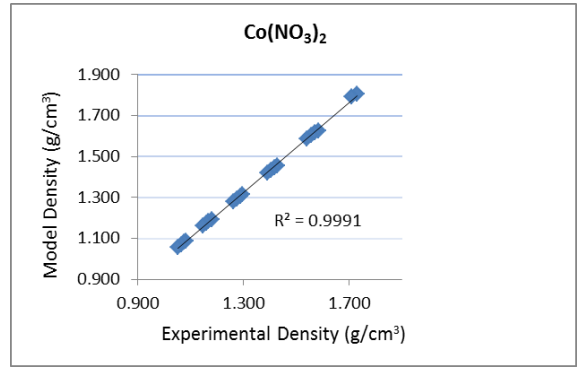


Figure 67: Plot of experimental vs. model density for  $\text{Co}(\text{NO}_3)_2$

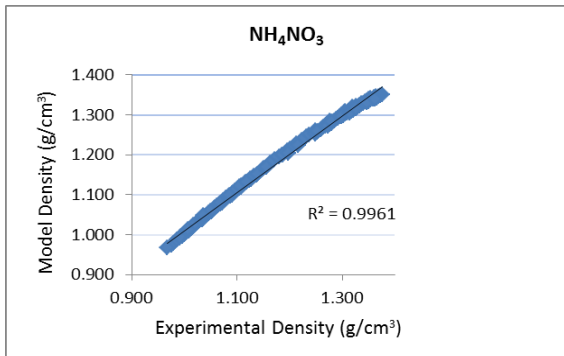


Figure 68: Plot of experimental vs. model density for  $\text{NH}_4\text{NO}_3$

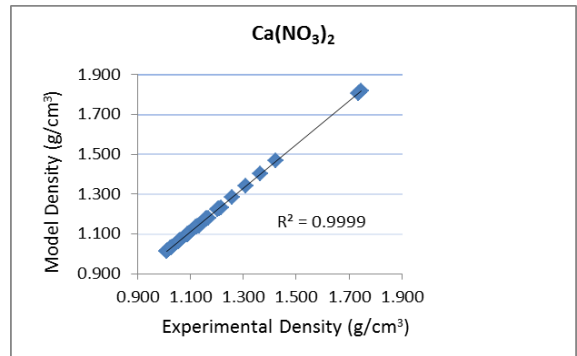


Figure 69: Plot of experimental vs. model density for  $\text{Ca}(\text{NO}_3)_2$

## APPENDIX F: GRAPHS FOR MIXED ELECTROLYTES

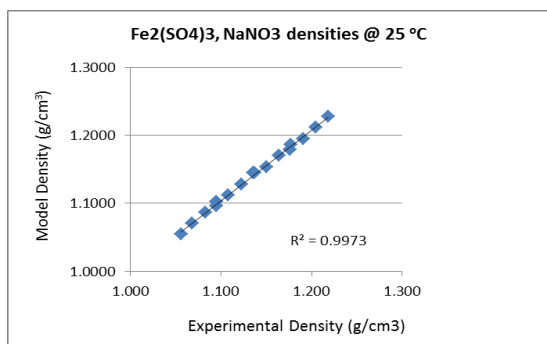


Figure 70: Plot of experimental vs. model density for Fe<sub>2</sub>(SO<sub>4</sub>)<sub>3</sub> and NaNO<sub>3</sub> at 25°C

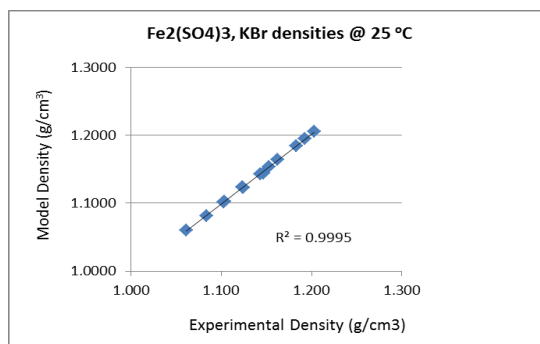


Figure 71: Plot of experimental vs. model density for Fe<sub>2</sub>(SO<sub>4</sub>)<sub>3</sub> and KBr at 25°C

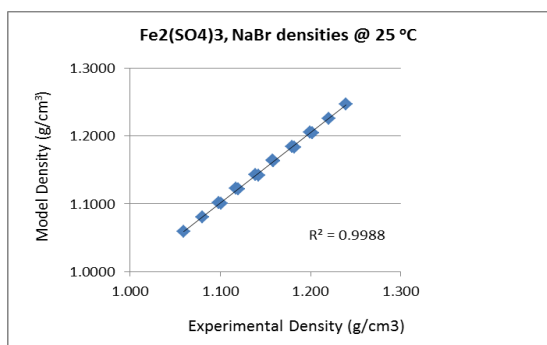


Figure 72: Plot of experimental vs. model density for Fe<sub>2</sub>(SO<sub>4</sub>)<sub>3</sub> and NaBr at 25°C

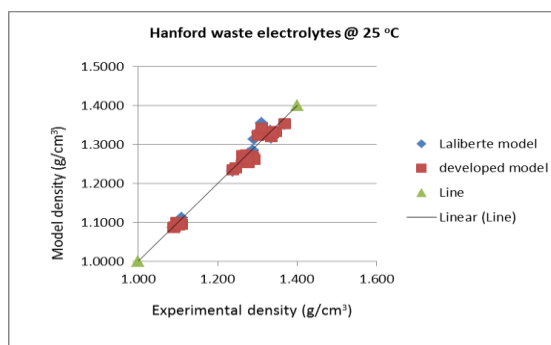


Figure 73: Plot of experimental vs. models density for Hanford waste solutions at 25°C

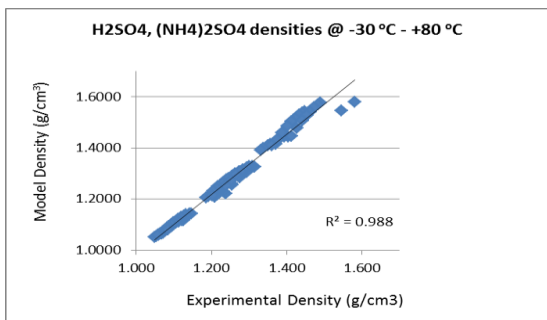


Figure 74: Plot of experimental vs. model density for  $\text{H}_2\text{SO}_4$  and  $(\text{NH}_4)_2\text{SO}_4$  at  $-30^\circ\text{C}$  to  $80^\circ\text{C}$

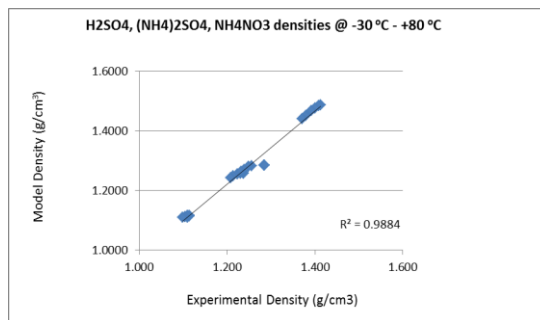


Figure 75: Plot of experimental vs. model density for  $\text{H}_2\text{SO}_4$ ,  $(\text{NH}_4)_2\text{SO}_4$  and  $\text{NH}_4\text{NO}_3$  at  $-30^\circ\text{C}$  to  $80^\circ\text{C}$

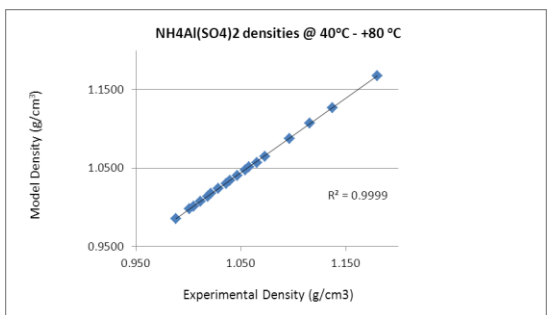


Figure 76: Plot of experimental vs. model density for  $\text{NH}_4\text{Al}(\text{SO}_4)_2$  at  $40^\circ\text{C}$  –  $80^\circ\text{C}$

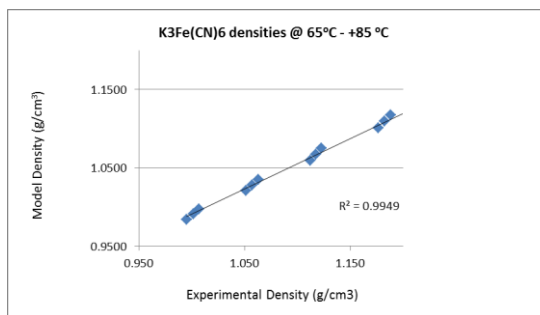


Figure 77: Plot of experimental vs. model density for  $\text{K}_3\text{Fe}(\text{CN})_6$  at  $40^\circ\text{C}$  –  $80^\circ\text{C}$